Pingos in Denmark

A comparison between pingo remnants in the Netherlands and circular depressions in South Jutland

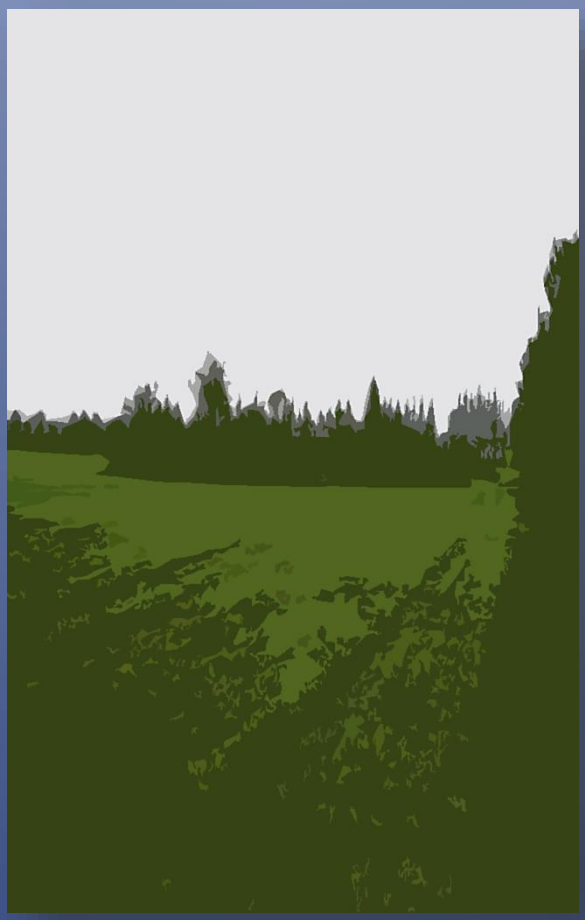

Utrecht University
Faculty of Geosciences
Department of Physical Geography
4th of July 2016

By: Machteld Caspers (3594254)
Supervisor: dr. W.Z. Hoek
Co-supervisor: PhD candidate Marjolein T.I.J. Gouw-Bouman

Abstract

Continuous and discontinuous permafrost zones extended over large parts of north-western Europe during the Weichselian glaciation, presumably as a result of hydrostatic groundwater pressure in partially frozen aquifers. This led to the formation of pingos regionally, in a fringe around the maximum extent of the ice sheet. In addition to the Netherlands, hardly any studies (Kolstrup, 1985) have focussed on the possible presence of pingo remnants further north, closer to the Sciandinavian Ice Sheet front, like Denmark. This study aims to present evidence of pingo remnants in Denmark and to compare this evidence with pingo remnants found in the Netherlands. A DEM and field survey in Southern Jutland revealed some of the characteristic geomorphological pingo remnant features, such as large isolated circular depressions. Moreover, the infill of one of the circular depressions appears to be comparable to that of pingo remnants in the Netherlands. The palynological results show a typical Late Glacial infill at the base. These first results are not conclusive, but they indicate that it is likely that some circular depressions in Denmark can be regarded as pingo remnants.

Table of contents

List of figures

List of tables

1. Introduction

Pingos are ice-cored hills that form under conditions of discontinuous permafrost, presumably as a result of hydrostatic groundwater pressures in partially frozen upper aquifers. The last couple of decades a lot has been written about pingos and pingo remnants (Flemal, 1975; Kolstrup, 1985; Mackay, 1986; Hoek, 1997; Harris & Ross, 2007). Nowadays, pingos are still present in artic regions where these conditions occur, like Canada, Alaska or Russia. However, hundreds of pingo remnants have been identified in other countries, many of them in the Netherlands. This can be explained by the regional glacial history of these areas; during the Weichselian Pleniglacial (tab. 1), (dis)continuous permafrost conditions were present in these regions.

Pingos can only remain stable for a certain amount of time, before they become unstable due to internal mechanisms, like growing too steep, or external factors, like climate change. Due to a temperature increase at the onset of the Lateglacial interstadial (Bølling-Allerød interstadial complex (Hoek, 2008), the ice in the pingos melted and the hills collapsed. This resulted in circular lakes, known as pingo remnants, with a maximum depth of the lakes approximately equal to the ice thickness of the decayed pingo (Flemal, 1975; Mackay, 1986; French, 2007). Over time, these residual lakes gradually fill up with gyttja, peat and aeolian deposits. The infill of these lakes can provide a high resolution paleo-climate/vegetation proxy record. This is due to the low risk of disturbances during and after sedimentation and the mostly anoxic condition at the bottom of the lakes, creating almost ideal preservation conditions (Flemal, 1975; Mackay, 1986; French, 2007).

Table 1: Overview of terminology and timing of Late Quaternary stadials (Berendsen, 2005).

Time period	Chrono-stratigraphic units		Age (ka)
Holocene		Early Holocene	11-9
Late Pleistocene	Weichselian	Late Weichselian (Late Glacial)	13 - 11
		Middle Weichselian (Pleniglacial)	73 - 13
		Early Weichselian (Late Glacial)	115-73
	Eemian		130-115
Middle Pleistocene	Saalien		370-130

Although permafrost was present in most of north-western Europe during the Late Weichselian, pingo remnants are only described in north-western European lowlands like the Netherlands. Hardly any studies (Kolstrup, 1985) have focussed on the possible presence of pingo remnants further north, closer to the old Sciandinavian Ice Sheet front, like Denmark. Permafrost conditions were also present in Denmark during the Weichselian, west and south of the maximum ice extent. Moreover, circular depressions similar to those in the Netherlands have been observed in Denmark.

This study aims to make a comparison between some of the numerous pingo remnants in the Netherlands and possible pingo remnants in Denmark, thereby highlighting the differences and similarities between the circular depressions in Denmark and the pingo remnants in the Netherlands. The hypothesis is that some of the circular depressions in Denmark which seem similar to pingo remnants of the Netherlands can be regarded as pingo remnants.

To test this hypothesis, fieldwork was done in the province Drenthe in the Netherlands and in the province South Jutland in Denmark. Circular depressions were selected using Digital Elevation Maps (DEMs), Google Earth and geological maps. The objectives of this research were:

- To compare the morphology, sedimentary characteristics and palynological profile of different pingo remnants in Drenthe, in order to find out if the timing of the decay of the pingos and the infill of the pingo remnants are different on a regional scale
- To determine if the suspected pingo remnants in Denmark actually are pingo remnants.
- If this is the case, to compare the timing of the decay of the pingos and paleoclimatalogical conditions during this decay with that of the pingos in the Netherlands.

This was accomplished by using literature, DEMs, coring, LOI analyses, constructing lithological cross sections and laboratory analyses.

In chapter 2 an overview will be presented of literature about different kinds of circular depressions and their many different origins. Chapter 3 will give the vegetation development during the Lateglacial and Early Holocene. Chapter 4 will describe the study areas, in which the Netherlands will be used as a key reference area for possible other pingo remnant sites in the Danish study area. Chapter 5 will describe the different methods used during this research and in Chapter 6 these results are presented. The results will be discussed in Chapter 7 and conclusions will be drawn in Chapter 8.

2. Circular depressions in former (peri)glacial environments

In this chapter a literature overview will be given of different kinds of periglacial features related to the formation of circular depressions over time. The main focus in this chapter lies on the periglacial feature pingos, of which the different types and different forms of creation will be discussed.

2.1 Pingos

Pingos are defined as "*ice-cored hills, typically conical in shape, that can persist and grow only in a permafrost area*" (Mackay 1998). Here, permafrost is defined as ground, both soil and rock, that remains at or below 0°C for two or more consecutive years. These conditions are present in two very different geographical regions; regions with high latitude and regions at a high altitude. The importance of permafrost becomes clear when taking into account that 23-25% of the land surface in the northern hemisphere is covered by permafrost (French, 2007), which is about 18.78 million km^2 or 16% of the global soil area (Khury et al., 2010). These numbers do not take into account the permafrost in the Alps, Andes or possible permafrost presence on Antarctica. Therefore, it is important to be precise when talking about permafrost and to make subdivisions. Permafrost is further classified into four zones of frozen ground fractions: continuous (90-100%), discontinuous (50-90%), sporadic (10-50%) and isolated (0-10%) (French, 2007). Pingos can occur in both continuous and discontinuous permafrost areas. They develop within the permafrost, below the active layer, making them an integral part of the permafrost (Gurney, 1998).

The name `pingo' is derived from the Inuit word pinga, which was and is used to describe ice-cored conical hills in the Mackenzie delta in Canada. The Inuit were not the only people naming such hills. There is a Russian equivalent for this word, `bulgunniakh', used by the Yakuts (Mackay, 1998; French, 2007; Yoshikawa, 2013). Pingos are one of the various types of frost mounds that occur in permafrost regions. Pingos can be distinguished from other frost mounds based on their structure and the character of the ice contained in the frost mound (French, 2007).

A well-developed pingo is a very distinct feature in a landscape, although pingo characteristics can differ somewhat between regions. A pingo can vary in size from a few meters to over 60 m in height and can be up to 300 m in width. The shape of a pingo is not always symmetrical; it can also be asymmetrical or elongated (French, 2007). Deviance from the symmetric shape is most pronounced in pingos on slopes (Flenal, 1975). The one thing that all pingos have in common is a centre of massive ice or icy sediment. All the previously mentioned features are influenced by specific limiting geomorphic and hydrologic conditions (French, 2007). In order to compare pingos, it

is important to not only look at the morphological features, but to also incorporate the different ways of pingo formation. However, all pingos require water pressure gradients, which provide water to form the ice core of the pingo (Gurney, 1998). This pressure gradient has to be large enough to overcome the geostatic overburden stress and deform the frozen soil (Harris & Ross, 2007). Based on these facts, pingos have been subdivided into open-system/hydraulic pingos and closed-system/hydrostatic pingos. The names hydraulic and hydrostatic are used more frequently since these names better describe the source of the pressure gradient which supplies water that initiates and sustains the pingos (Mackay, 1979).

2.1.1 Hydrostatic (closed-system) pingos

Both Müller (1959) and Mackay (1962) were the first to describe exactly what a closed-system pingo was (Gurney, 1998; French, 2007). Mackay (1979) later changed the name of this type of pingo to hydrostatic pingo (fig. 1). However, in 1938 Porsild was the first to suggest the basic concept for hydrostatic pingos (Porsild 1938; Gurney, 1998*); "local upheaval due to the expansion following the progressive downward freezing on all sides of a body or lens of a semi-fluid mud or silt enclosed between bedrock and the frozen surface soil"*. This definition has changed over time with increasing understanding and knowledge. A hydrostatic pingo is nowadays defined as *"a pingo that originates from pore-water expulsion, caused by permafrost aggradation beneath the bottom of drained lakes that are underlain by saturated sands"* (French, 2007). Most of today's understanding of hydrostatic pingos is based on the research of Ross Mackay on pingos in the Mackenzie Delta, Canada (Mackay 1962, 1972, 1979). Here, permafrost develops in a deltaic sequence of sand, silt and clay. Thus, surface water can gather to form pools and lakes during summer. When the winter ice becomes thinner than the depth of these lakes, the mean temperature of the lake bottom will rise to above zero. This will cause a thaw bulb or talik to form in the permafrost beneath the lake. As the lake drains later on, the talik will be refrozen, which leads to permafrost advancing downwards from the surface of the paleo-lake and inwards from the sides (Harris & Ross, 2007). If there is unfrozen sand present in the talik, and this sand freezes, the volume will increase by 9% (phase change). This then results in 9% pore water expulsion ahead of the advancing freezing front. The pore water then migrates under hydrostatic pressure to the zone with the least amount of stress, which is usually below a still existing pond in a paleo-lake basin. After this, freezing from the surface downwards will start the formation of the first ice of the pingo ice centre (Harris & Ross, 2007). Once the freezing has begun, the ice that starts the formation of the pingo will not increase significantly in diameter.

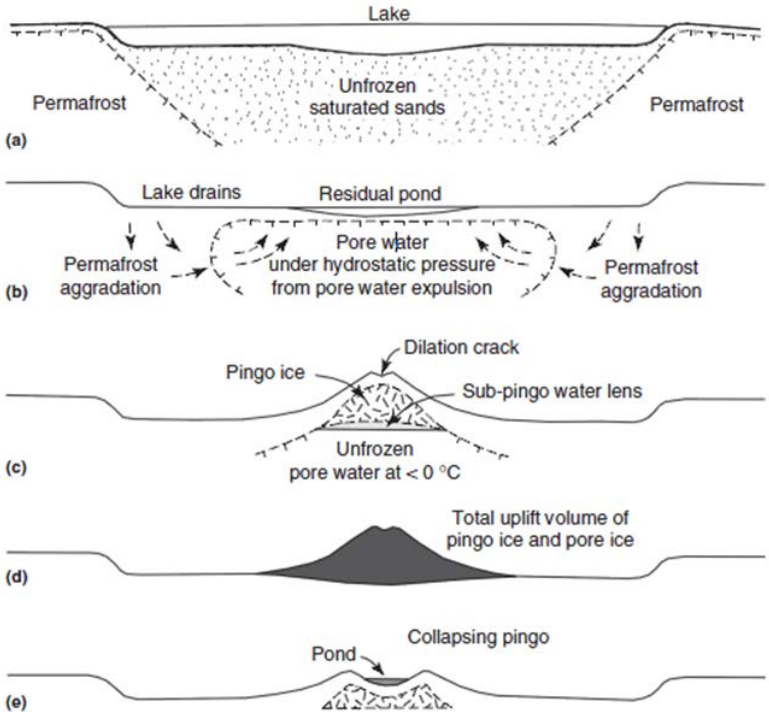

Figure 1: Formation of a hydrostatic (closed system) pingo (Harris & Ross, 2007)

The increasing volume of the hydrostatic pingo is mostly derived from the raising of the surface, of which the maximum elevation is at the centre of the pingo mound (Mackay, 1998; Harris & Ross, 2007). When a relatively high concentration of hydrostatic pingos is present, it is usually related to a couple of favourable conditions: (1) thick permafrost, (2) large areas that are underlain by coarse-grained sediment and (3) a large number of thermokarst lakes that are easily drained (French, 2007). Because the presence of all these contributors in one geographic location is very rare, it makes it relatively easy to identify a hydrostatic pingo (Yoshikawa, 2013).

According to Gurney (1998) the size of a hydrostatic pingo is connected to the area of the (paleo)lake the talik grows underneath, since this is the determining factor of the volume of the talik itself. The average diameter of a hydrostatic pingo is approximately 200 m, but can grow up to 600 m. The sides of a hydrostatic pingo usually have a slope around 34° to 38°, since this is approximately the angle of repose of sand, which is the major component of the unconsolidated sediment in which hydrostatic pingos form (Gurney, 1998).

2.1.2 Hydraulic (open-system) pingos

Hydraulic pingos (fig. 2) are defined as pingos that develop at locations where intrapermafrost (between permafrost) or subpermafrost (below permafrost) groundwater is transported to the surface by means of artesian pressure (Müller, 1959). In contrast to hydrostatic pingos, hydraulic pingos are usually isolated features or present in small groups within the same locality (French,

2007). Moreover, many hydraulic pingos not only occur in continuous permafrost areas, but also in areas with thin and/or discontinuous permafrost. They are most common in areas with topographic relief, for example on lower valley sides or at the bottom of valleys (Harris & Ross, 2007). Most locations of hydraulic pingos are clearly related to groundwater seepage. During winter, small springs and icings can form on the flanks of the hydraulic pingos (French, 2007).

Although a lot of studies have investigated pingos, there exists no growth data regarding hydraulic pingos. It is assumed that hydraulic pingos grow through ice injection (French, 2007). However, pingo growth solely due to ice injection is an unstable situation. If this is the case, there has to be a long-term balance between the factors: (1) water pressure, (2) overburden strength and (3) rate of freezing (Mackay, 1973). These factors may change independently of each other, making it very difficult to maintain a long-term balance (French, 2007). This implies that injection is not the only factor controlling the growth of hydraulic pingos. Hydraulic pingo growth probably requires some ice segregation as well (French, 2007).

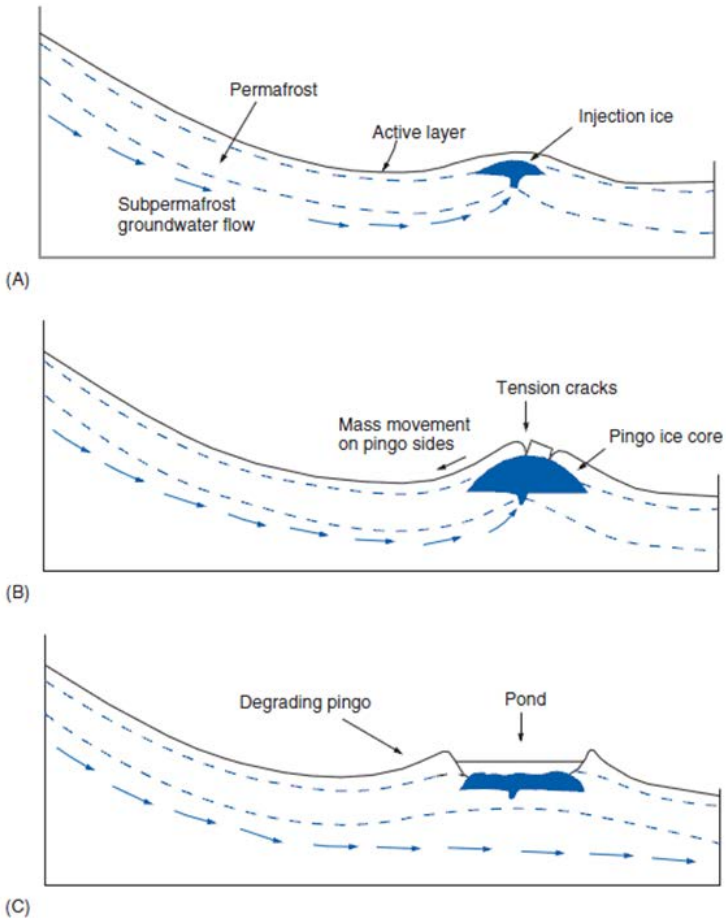

Figure 2: Formation of a hydraulic (open-system) pingo (Yoshikawa, 2013)

According to Gurney (1998) sizes and shapes of hydraulic pingos are not that different from hydrostatic pingos. One of the larger observed hydraulic pingos (Müller, 1959) has a diameter of 350 m and a height of 38 m, which is comparable to the morphological parameters of hydrostatic pingos. The angle of repose is also similar. The biggest morphological difference is the overburden material. Most hydrostatic pingos are composed of fluvial material, while hydraulic pingos often have overburdens of rock, such as (micaceous) sandstone (Gurney, 1998).

2.2 Pingo failure and decay

Although pingos start as stable permafrost features, they will eventually become unstable and decay. This can be caused by limiting climatic factors (Mackay, 1988; Gurney, 1998) or, more common, it is related to mechanics (Mackay, 1998; Gurney, 1998). The onset of pingo decay is usually initiated by radial dilation cracks and concentric cracks, which will eventually result in mechanical failure of the pingo overburden. Not only overburden failure of the pingo, but also creeping, faulting and ice-wedging cause deformation of the pingo (Mackay 1998; Harris & Ross, 2007). Slumping and solifluction also take place and transport sediment off the pingo to the base of the mound where it accumulates (Harris & Ross, 2007). When the pingo ice is exposed the decay of the pingo starts with the thawing of ice, which leads to the formation of a summit pond. This summit pond then provides a positive feedback on thawing, which accelerates. After the thawing is complete, a pond is left where the pingo used to be. This pond is characterized by a raised rim/ridge/rampart of sediment circling it as a result of mass movement (Harris & Ross, 2007).

2.2.1. Mechanically induced failure

There are three types of mechanical failures: (1) summit/dilation failure, (2) circumferential failure and (3) hydrofractures and sub-pingo peripheral failure. When a pingo reaches the height of several meters, summit cracks/dilation cracks are often formed through the dilation of the pond bottom (Mackay, 1998). These cracks continue downward through the overburden of the pingo, usually all the way into the ice. As the pingo grows so do the dilation cracks, becoming flat-floored trenches and V-shaped gullies. When the dilation cracks widen, the overburden at the bottom of the dilation cracks becomes thinner. The widening of the dilation cracks continues until some of the ice of the pingo becomes exposed to thaw and a `pingo crater' is created. The stresses that cause the dilation cracks are related to mechanical pingo growth, making it possible for dilation cracks to form at any point in time (Mackay, 1998).

Circumferential failure is a result of a decline in the increase of circumference of a pingo at any given height through radial dilation cracks (fig. 3). The radial dilation cracks are formed after summit dilation cracks and are usually orthogonal. These cracks can be filled with surface water to form dilation crack ice. This will eventually lead to the failure of the pingo (Mackay, 1998).

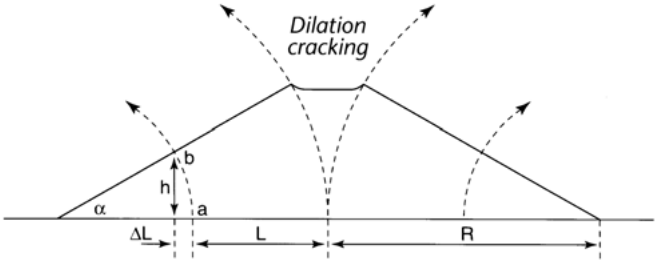

Figure 3: Dilation cracking in a pingo (Mackay, 1998)

Hydrofractures and sub-pingo peripheral failure mostly refers to the hydrofractures that happen when the "*fluid pressure within a sub-pingo water lens exceeds the tensile strength of the enclosing frozen material plus the least compressive principal total stress with compression positive"* (Mackay, 1998). The stress in the sub-pingo water depends on local features like pingo shape, material, and ground temperature. When these features fail, hydrofractures arise (Mackay, 1998). Most of these failures occur at the periphery of the sub-pingo water lens. From here, the fractures extend to all sides of the entire pingo. This will eventually lead to mechanical failure (Mackay, 1998).

2.2.2 Climatic failure

Literature on this topic is sparse. Although climatic failure is mentioned in literature, as by Gurney (1998), who mentions that pingo collapse can be related to climatic amelioration, the only author who explains this concept in more detail is Mackay (1988). Mackay (1988) also refers to "*some publications in the Soviet Union"*, but no sources were mentioned. Mackay (1988) explains that pingos that grow in permafrost areas usually collapse under mechanical failure when radial dilation cracks and concentric cracks have formed. However, the mean annual temperature is also a limiter of pingo growth and cause of collapse. These temperatures can be expressed in various ways, of which the mean annual air temperature (MAAT), mean annual ground surface temperature (MAST) and the mean annual ground temperature (MAGT) are of significance. The relationship between climate, pingo growth and temperature (MAGT) are depicted in fig. 4, after Mackay (1988). Scenario a shows the more common climate scenario of climate warming. During climate warming, only small pingos can grow to full size and reach the maximum pingo growth curve, after which they quickly collapse. Scenario b shows that as long as the climate remains stable, pingos of all sizes can start to grow until they eventually collapse due to mechanical failure. Scenario c shows a climate cooling in which pingos of all sizes can reach their maximum growth potential before mechanical failure occurs. Mackay (1988) further states that due to the many temperature variabilities and pingo dynamics, no reliable temperature limits can be given to pingo growth. The non-climatic factors, pingo size, talik

size and permafrost thickness, have too much influence on pingo dynamics. This makes it impossible to create a simple mathematical relationship between temperature and pingo collapse (Mackay, 1988).

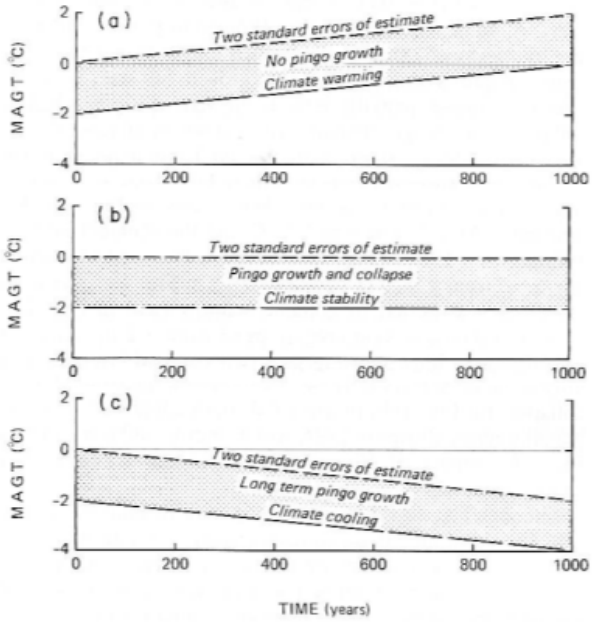

Figure 4: Relationship pingo collapse and temperature; a) climatic warming scenario, b) climatic stable scenario, c) climatic cooling scenario (Mackay, 1988)

2.3 Pingo remnants

Each pingo has a preservation potential according to Gurney (1998) which will determine whether the pingo will remain a geomorphological feature in the future as a pingo scar or as a pingo remnant. The preservation potential depends on the size of the ramparts, the central depression and the material from which they are constructed (Gurney, 1998). Nowadays, pingo remnants are evidence of the presence of (Pleistocene) permafrost at a certain moment in time. However, pingos are/were not the only frost mounds in existence and not all of these frost mounds require the presence of permafrost (French, 2007; Harris & Ross, 2007). Therefore, it is very important to identify pingo remnants correctly and to, when a circular depression is observed in the field, first call it a *"ramparted ground ice depression"* (Bryant & Carpenter, 2011) before making a connection to the genesis (Harris & Ross, 2007). According to French (2007) pingos are "*not common features in a periglacial landscape and only abundant in some geographic areas".*

Table 2: Pingo classification table.

	Mackay (1987; 1988; 1998)	Gurney (1998)	Harris & Ross (2007)	De Gans (1988)	Flemal (1975):
Dimensions & shape	*"The maximum topographic relief is about 1.5 m"*		*"Enclosed depressions surrounded by annular ring ridges or ramparts".*	*"Average depth as measured from the land surface during pingo growth is 4-5 m, with extremes of 1,5 m and 17 m".*	
	"Circular (mostly), elongated or crescent-shaped (which are more likely to rupture than circular pingos) depressions".			*"The diameter of the pingo scars ranges between 25 m and 350 m. Although, in the Netherland a minimum of approximately 100 m is applicable".*	
Rampart & depression	*"The volume of the rampart should be approximate that of the enclosed depression from which the rampart material was derived. When a volume approximation is made, it should still be considered that material loss might occur from processes such as deflation or stream transport and material might be gained due to in situ accumulation of organic material".*	*"A centrally located summit crater, with circular or oval ramparts surrounding a central depression, which may or may not contain a pond in summer".*		*"Sometimes the rampart is completely absent".*	*"The central depression itself often contains a lake, pond, or bog, which is the site of secondary deposition. This deposition may result from the accumulation of organic debris, wind-blown debris, debris washed in from adjacent higher ground, or debris welled up from below by rising groundwater".*
				"The depression may be filled with a sequence of sediments: redeposited overburden and rampart material, lake deposits such as laminated silt, clay, detritic gyttja and gyttja followed by peat".	
Occurrence			*"They are frequently found in clusters, and in western Europe they are sited on valley bottoms, slope–valley interfaces, and in some plateau locations".*	*"Either found in loose groups or as solitary occurrences".*	*"Considerable variation from the ideal may occur. The regular outline may be disturbed by interfering successive generations of pingos".*
				"Pingo scars occur on flat ground or on slopes with a gradient up to 5°".	
				"Pingo scars are accompanied by other permafrost phenomena".	
Other characteristics	*"Signs of radial dilation cracking, the casts of dilation-crack ice, and extensions of radial cracks into the surrounding area".*				*Pingo scars may occur in any type of substrate. However, they are most prevalent in areas where the substrate is wet and particularly at places of emerging ground water".*
	"If casts resembling small to very large ice wedge casts cross a rampart at right angles, a pingo origin would seem likely".				

2.4 Alternative explanations

Although most applied identification criteria for pingo remnants concur with each other, some of the mentioned identification criteria are also applicable to other geomorphological features.

2.4.1 Pitted Sandar with kettle holes

Although pitted sandar is the name most used in literature, many others also refer to the same phenomenon: kettled sandar, kettled outwash plain or dead ice hollow. These dead ice hollows are created when isolated buried blocks of ice from the glacier melt-out, thereby creating the mentioned hollows (Benn & Evans, 2010). According to Benn & Evans (2010), two processes are mainly responsible for this:

(1) Differential ablation of the glacier snout causes ice to detach from the glacier.

(2) Flood water transport of icebergs onto the sandar.

In both scenarios, glaciofluvial sediment may partially or completely be deposited on top of the ice blocks and bury them (Benn & Evans, 2010). Parts of ice-marginal sandar may accumulate supraglacially. After the ice melts pitted zones can be created here. This phenomenon can happen along deglaciated valleys where overlapping fans are prograded sequentially (Benn & Evans, 2010).

Other features can accompany the pitted sandar, namely rims. These rims are a result from the ice melts and can produce boulder ring structures anywhere between 3-40 m in diameter, surrounding the pitted sandar depression (Benn & Evans, 2010). Benn & Evans defined four different types of pitted sandar (fig. 5);

(1) "*A normal kettle hole"* without any surrounding structures

(2) "*A rimmed kettle hole*" with a till in the central depression. The rim consists of low-amplitude boulders.

(3) "*A crater kettle"* has a thick diamiction layer in the pit which extends towards the sides where it forms a thick boulder-covered diamiction rim around the depression.

(4) "*A till-fill kettle"* is a filled in pitted sandar by the sediment that was situated on top of the ice block, resulting in a mound of diamiction filling in the depression. No rim is present.

The depressions that are left after the melting of buried dead ice masses visually resemble a pingo remnant

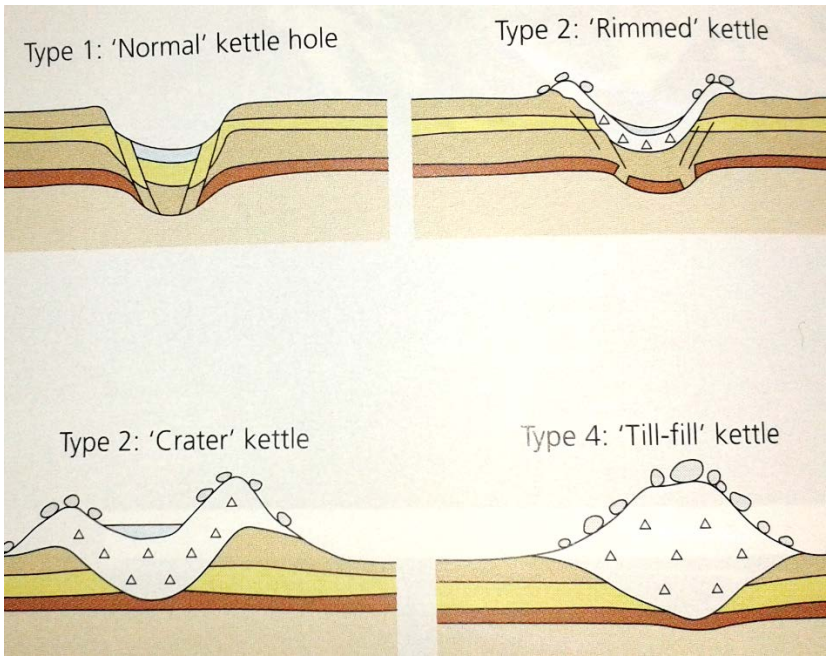

Figure 5: Different types of pitted sandar (Benn & Evans, 2010)

2.4.2 Palsas

Palsas were originally defined as a "*hummock rising out of a bog with a core of ice"* (Seppälä, 1972). Nowadays they are defined as peaty permafrost mounds with a core of alternating layers of segregated ice and peat or mineral soil (French, 2007). The height of a palsa is typically somewhere between 1-7 m and the width is usually less than 100 m (French, 2007). However, Goodie (2013) defines palsas with larger dimensions: a dome shaped palsa can have a maximum diameter of 150 m, with a height of up to 12 m and a longitudinal palsa can be up to 500 m long and 6 m heigh. The identification criteria used for palsas are their build, their location in wetlands/fens/bogs and that ice segregation is the main growth contributor (French, 2007). Although these criteria work in current periglacial environments, palsa remnants can have the same dimensions as pingo remnants. Furthermore, when no rampart is present; pingos' and palsas' (remnant) characteristics are very similar.

2.4.3 Small perennial ice-cored mounds

Pingos can be defined as *"a perennial frost mound consisting of a core of massive ice, produced primarily by injection of water, and covered with soil and vegetation"* (Harris et al, 1988). However, this description could also be applied to small perennial frost mounds (Mackay, 1998). These small perennial frost mounds grow in the same environment as pingos; *"in sedgy drained lake flats near pingos in the freeze-back period by the injection of water into the bottom of the active layer"* (Mackay, 1998). Therefore it has long been proposed (Müller, 1945) to add a distinction of relative large dimensions to the definition of pingos. Mackay (1998) added the permafrost condition to the pingo definition. Furthermore, to complicate matters, small perennial ice-cored frost mounds can

grow at the periphery of a pingo by hydrofracturing and rupture with intrusion of water into the permafrost (Mackay, 1998). This makes it possible for these small perennial ice-cored mounds to exist in permafrost regions, even though permafrost is not necessarily for their formation. These perennial frost mounds are divided into two groups: the seasonal-frost mounds and the hydrolaccoliths and other frost-induced mounds (French, 2007).

Seasonal-frost mounds can develop when freezing of the active layer restricts perennial discharge from permafrost and small mounds develop at the location of the groundwater discharge (French, 2007). The small seasonal-frost mounds are characterized by a height of 1–4 m (French, 2007). However, other authors have different ideas about the dimensions of the small seasonal-frost mounds; De Gans (1988) claims a maximum height of 8 m, while Mackay (1998) states a maximum height of 2 m. Generally, small seasonal–frost mounds are smaller than pingos (French, 2007; De Gans, 1988; Mackay, 1998). The small seasonal-frost mounds are sometimes confused with palsas, but the main difference is that palsas result from ice segregation while seasonal-frost mounds result from ice injection (French, 2007).

Hydrolaccoliths and other frost-induced mounds are features in tundra landscapes that are considered to be different from pingos mainly based on their size and location. While pingos usually have a diameter of a couple of hundred meters, these frost-induced mounds do not exceed 50 m in diameter and are located within the active layer. The origin of these features is not clear (French, 2007).

3. Vegetation development

3.1 The Netherlands

Various authors have described the vegetation development of the Netherlands during the Lateglacial and Early Holocene (Van Geel et al., 1989; Hoek, 1997). The development of Dutch vegetation has been separated into different pollen zones and attached to an uncalibrated radiocarbon timescale (tab. 3). A brief description of these zones will be given here, mostly based on Hoek (1997). Van Geel (1989) used slightly different criteria for zonation and applied different naming.

Table 3: Naming and timing of biozones, Hoek (1997, 2008)

Biozone	^{14}C years BP	Age (ka)	Zone
(first part of) Boreal	9500-	9-	5
Preboreal	10150-9500	11-9	4
Younger Dryas stadial	10950-10150	13-11	3
Allerød interstadial	11900-10950		2
Older Dryas stadial	12100-11900		1c
Bølling interstadial	12450-12100		1b
Oldest Dryas/Late Pleniglacial stadial	12900-12450	-13	1a

3.1.1 Zone 1

Pollen zone one has been defined by van Geel et al. (1989) and Hoek (1997) as having a relatively low percentage of arboreal pollen and a high percentage of upland herbs. "*Herbaceous plant communities and dwarf shrubs developed as a result of temperature rise"* (Hoek, 1997). It concerns zone 1a-1c (tab. 4) from 12900-11900 ^{14}C years BP otherwise known as the (a) Oldest Dryas (Hoek, 1997) or Late Pleniglacial (Hoek, 2008), (b) Bølling and (c) Older Dryas.

Subzone 1a (12900-1245014C years BP) is characterized by high *Artemisia* values and is followed by subzone 1b (12450-12100 14C years BP). Subzone 1b is characterized by an increase in Arboreal Pollen (AP), especially *Betula*. Subzone 1c (12100-1190014C years BP is marked by a more

open vegetation; more Non Areal Pollen (NAP), decreasing *Betula* pollen percentages and increasing *Salix* pollen percentages (Hoek, 1997).

3.1.2 Zone 2

Pollen zone two represents the vegetation of the Allerød from 11900-10950 ^{14}C years BP (Hoek, 1997). A subdivision can be made into subzone 2a and 2b, of which subzone 2a sometimes can be divided as well into zone 2a1 and 2a2. Zone two is characterized by an open *Betula* forest and *Pinus* forest (Hoek, 1997) (tab. 4).

Subzone 2a (11900-11250^{14}C years BP) is characterized by increasing, relatively high *Betula* pollen percentages and increasing AP percentages. Relatively large decreasing NAP percentages and small decreases in *Salix* pollen may also occur. The differences between 2a1 and 2a2, which sometimes occur, are slight decreasing *Betula* pollen and *Juniperus* pollen percentages and slight increasing *Pinus* pollen percentages. Subzone 2b (11250-10950^{14}C years BP) starts at the high increase in *Pinus* pollen percentages (Hoek, 1997).

Table 4: Regional pollen zonation scheme for the Lateglacial and Early Holocene, the Netherlands (Hoek, 1997)

zone level1	sub-level2	sub-level3	Zone Code	pollen percentage characteristics
5	5	5	5 0 0	*Pinus* ↑↑
4	4c	4c	4 3 0	*Betula* ↑, *Populus* ↑
4	4b	4b	4 2 0	*Betula* ↓, *Gramineae* ↑, AP ↓
4	4a	4a	4 1 0	*Betula* ↑↑, *Juniperus* ↑, NAP ↓
3	3b	3b	3 2 0	*Empetrum* ↑
3	3a	3a	3 1 0	*Pinus* ↓, *Betula* ↓, AP ↓, NAP ↑
2	2b	2b	2 2 0	*Pinus* ↑↑
2	2a	2a2	2 1 2	*Betula* ↓, *Pinus* ↑, *Juniperus* ↓
2	2a	2a1	2 1 1	*Betula* ↑↑, *Salix* ↓, AP ↑↑, NAP ↓↓
1	1c	1c	1 3 0	*Betula* ↓, *Salix* ↑, *Juniperus* ↑, NAP ↑
1	1b	1b	1 2 0	*Betula* ↑, AP ↑
1	1a	1a	1 1 0	*Artemisia* ↑
Late Pleniglacial (LP)				

3.1.3 Zone 3

Pollen zone three can be subdivided into two different parts: 3a and 3b. Together these parts represent the equivalent of the Late Dryas 10950-10150 ^{14}C years BP. Zone three marks the halt in

the development towards a denser vegetation cover; both *Pinus* and *Betula* forest diminish in size (Hoek, 1997)(tab. 4).

Subzone 3a (10950-10550 ^{14}C years BP) is characterized by diminishing forests and the development of herbaceous plant communities, this is also reflected in decreasing AP percentages and increasing NAP percentages. Subzone 3b (10550-10150^{14}C years BP) is marked by the development of *Empetrum nigrum*, mostly in the northern Netherlands (Hoek, 1997).

3.1.4 Zone 4

Pollen zone 4 (10150-9500 ^{14}C years BP), the Preboreal, marks the onset of the Holocene and is subdivided into three different subzones (Hoek, 1997)(tab. 4).

Subzone 4a (10150-9950 ^{14}C years BP) is marked by a large increase in *Betula* pollen percentages, an increase in *Juniperus* pollen percentages and a decrease in NAP percentages. Subzone 4b (9950-9750 ^{14}C years BP) has a more open vegetation and is characterized by an increase in Gramineae (Poaceae) pollen percentages and a decrease in *Betula* pollen percentages. During subzone 4c (9750-9500 ^{14}C years BP), the *Betula* forest expands and *Populus* pollen percentages increase (Hoek, 1997).

3.1.5 Zone 5

Pollen zone 5 starts at 9500 ^{14}C years BP. and starts at increasing *Pinus* pollen percentages (tab. 4), as the *Pinus* forest expands and becomes denser due to rising temperatures (Hoek, 1997).

3.2 Denmark

Iversen (1973) made an overview of the vegetation development in Denmark since the last glacial. In contrary to Hoek (1997), no zones were established by Iversen (1973), but an general overview of the trends in the percentages of the most common pollen of that time was given. Most trends agree with Hoek (1997). Therefore, it is logical to apply the Dutch zonation on the Danish pollen diagrams. Mortensen et al. (2011) made a pollen assemblages zonation framework for the vegetation history at the end of the last glacial, at Slotseng (Denmark). This framework from Mortensen et al.(2011) was also consulted, and compared with the Danish pollen diagrams, before applying the Dutch zonation.

4. Study area

The study area is the NW European lowlands, with a focus on the province Drenthe in the Netherlands and the province South Jutland in Denmark. Both focus areas have a similar (peri)glacial history during the Saalien (fig. 6) and Weichselian (fig. 7).

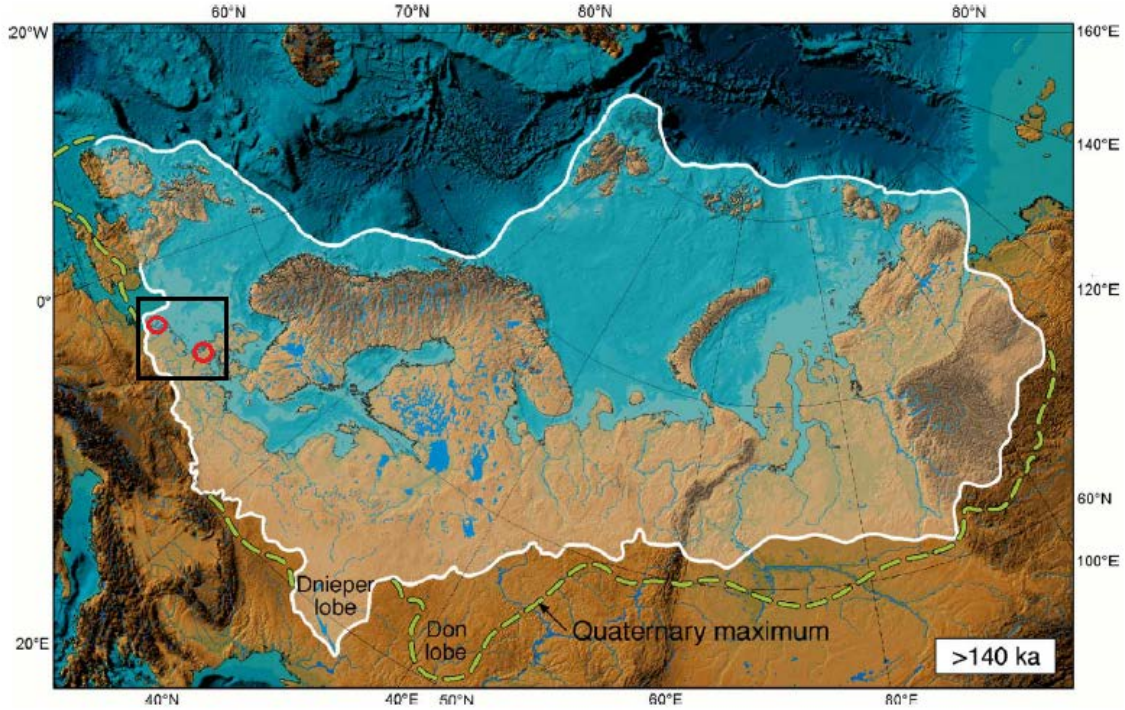

Figure 6: Marked approximation of the study area (black box), focus areas (red circles) and glacial configuration of Scandinavian Ice Sheet during the Late Saalian (white markings), after Svendson et al. (2004)

4.1 Glacial history

4.1.1 Saalian

The Saalian is the second to last glacial period (tab. 1), it is approximated to have taken place between 370-130 ka. The exact ages are hard to determine due to lack of datable continental deposits. This can be explained by lack of deposition due to erosion during the last glacial period. Most ages are derived from glacial related features that were not eroded during the last glacial period or from indirect, deep sea evidence (Mulder et al., 2003).

The Scandinavian Ice Sheet (SIS) expanded across Europe (fig. 6), resulting in a 120-140 m sea level drop. Large parts of Northern Europe were covered by land ice, forcing rivers to change direction towards the south-west. Scandinavia, including Denmark was completely covered by the ice, but the Netherlands was only partly covered with land ice, creating many moraine ridges in the centre of the Netherlands (Mulder et al., 2003).

4.1.2. Weichselian

The SIS reached its maximum extent in Denmark around 22 kyr BP (Houmark-Nielsen & Kjaer, 2003). Although other sources put the maximum ice extent (fig. 7) during the Last Glacial Maximum (LGM) at 20 ka (Ehlers & Gibbard, 2004; Landvik et al., 1998; Svendson et al, 2004). The Main Stationary Line (shortened to MSL by Houmark-Nielsen (1999) in fig. 8) is an indicator of how far the SIS extended towards the west during the Weichselian (Houmark-Nielsen, 2007). The Main Stationary Line reached as far as halfway through South Jutland, Denmark. The boundary is based on several ice marginal segments of suspected different ages (Houmark-Nielsen & Kjaer, 2003). The Scandinavian Ice Sheet did not reach the Netherlands during the Weichselian. However, the Netherlands was affected by the SIS. Due to the ice extension and the low temperatures, water levels dropped during the Weichselian, including that of the North Sea. This caused the climate to become more continental. The colder, glacier climate became relatively warmer during interstadials and cold during the stadials, which can be seen in the pollen record. During the Early and Late Pleniglacial (tab. 2) vegetation was scarce, the ground was mostly frozen (discontinuous permafrost) and aeolian sand transport took place (Berendsen, 2005).

After the LGM, a deglaciation sequence from 20-15 kyr BP took place (Houmark-Nielsen & Kjaer, 2003). By 19 kyr BP the western and south-western margins (Southern Jutland) of the SIS were retreating. Due to isostasy, transgression took place and regressional coast lines, on the east side of Denmark, followed the retreat of the glacier (Houmark-Nielsen & Kjaer, 2003). Other sources (Björck & Möller, 1987; Björck, 1995) claim that the deglaciation continued rapidly until at least 12 kyr BP.

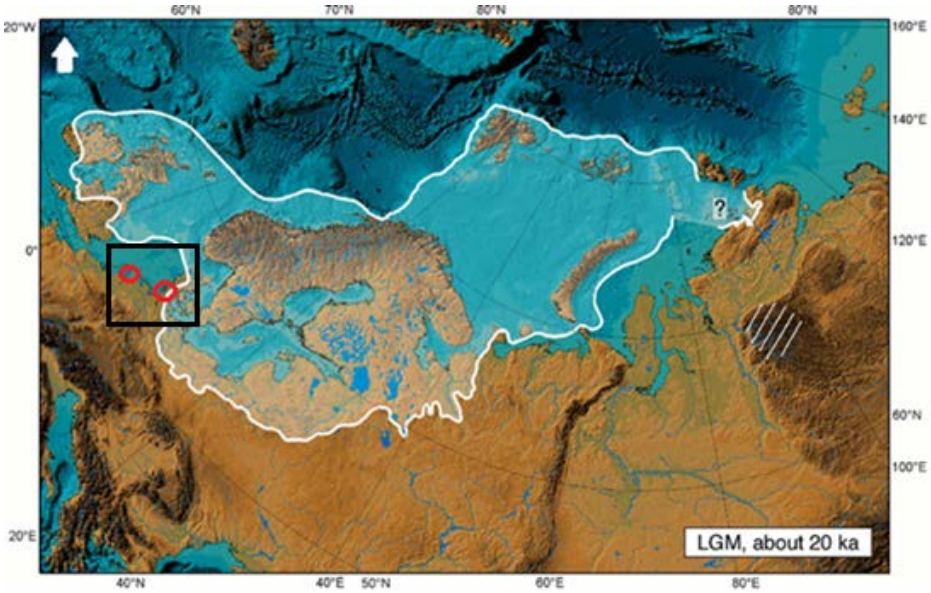

Figure 7: Marked approximation of the study area (black box), focus areas (red circles) and glacial configuration of Scandinavia during the LGM (white markings), after Svendson et al. (2004)

4.2 Location and local deposits

4.2.1 Drenthe, the Netherlands

Both of the Dutch coring sites are located in the middle-west of the province of Drenthe, which is known for its high density of pingo remnants (fig. 8) (Bruijn, R. D., 2012; Ruiter, A. S., 2012).

Drenthe is part of the northern sand area in the Netherlands, which also covers parts of the provinces Overijssel, Friesland and Groningen. The northern boundary of the area is positioned at the point where the Pleistocene sand deposits dip under the Holocene deposits, consisting of marine and/or peat deposits. This area is also referred to as the Drenthe Plateau (Berendsen, 2005).

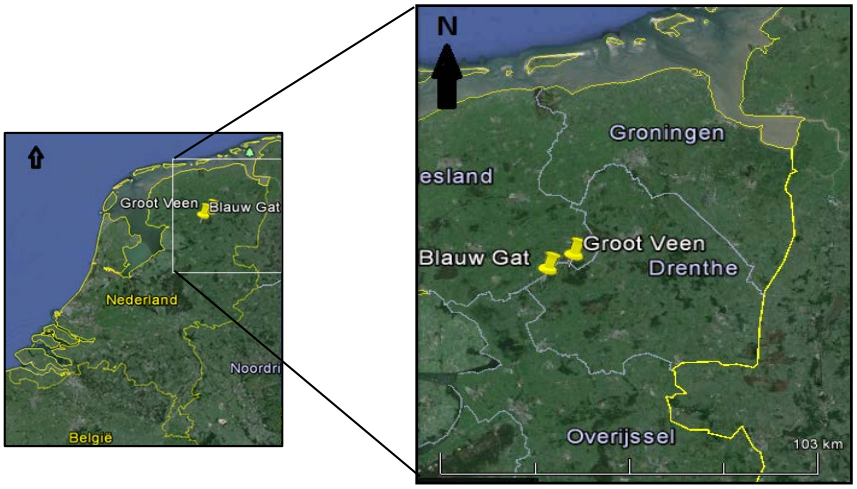

Figure 8: Fieldwork area the Netherlands, Drenthe, (Google Earth)

During the Early Weichselian, the Netherlands was characterized by an open park landscape. Terrestrial sediments from this period are mainly of aeolian origin and often display cryoturbation marks (Mulder et al., 2003).

The Middle Weichselian (Pleniglacial) starts with a strong temperature drop, resulting in the disappearance of connecting forests and the development of a tundra landscape and many bare stretches of land. Permafrost developed shortly after this. This period is marked by strong erosion; the wind eroded the surface due to scarce vegetation cover and rivers incised into the subsurface. During the latter part of the Middle Weichselian river incision decreased and fluvial sedimentation resumed. The deposits from the Middle Weichselian are mostly of aeolian or fluvio-periglacial origin (Mulder et al., 2003).

The Late Weichselian is characterized by an overall increase in temperature, rapidly changing vegetation, melting of land ice and rising sea levels. Soil formation occurred during the warmer periods in the Late Weichselian in the cover sands, but cryoturbation and river dune formation also occurred during colder periods (Mulder et al., 2003).

4.2.2 South Jutland, Denmark

The two Danish coring sites are located in Denmark's most southern province: South Jutland (fig. 9a). The sites are about 60 km apart and are both positioned west of the Main Stationary Line (MSL) (fig. 9b). Most of the Quaternary deposits overly Cretaceous chalk or Cretaceous clays and silts (Pedersen, 1989).

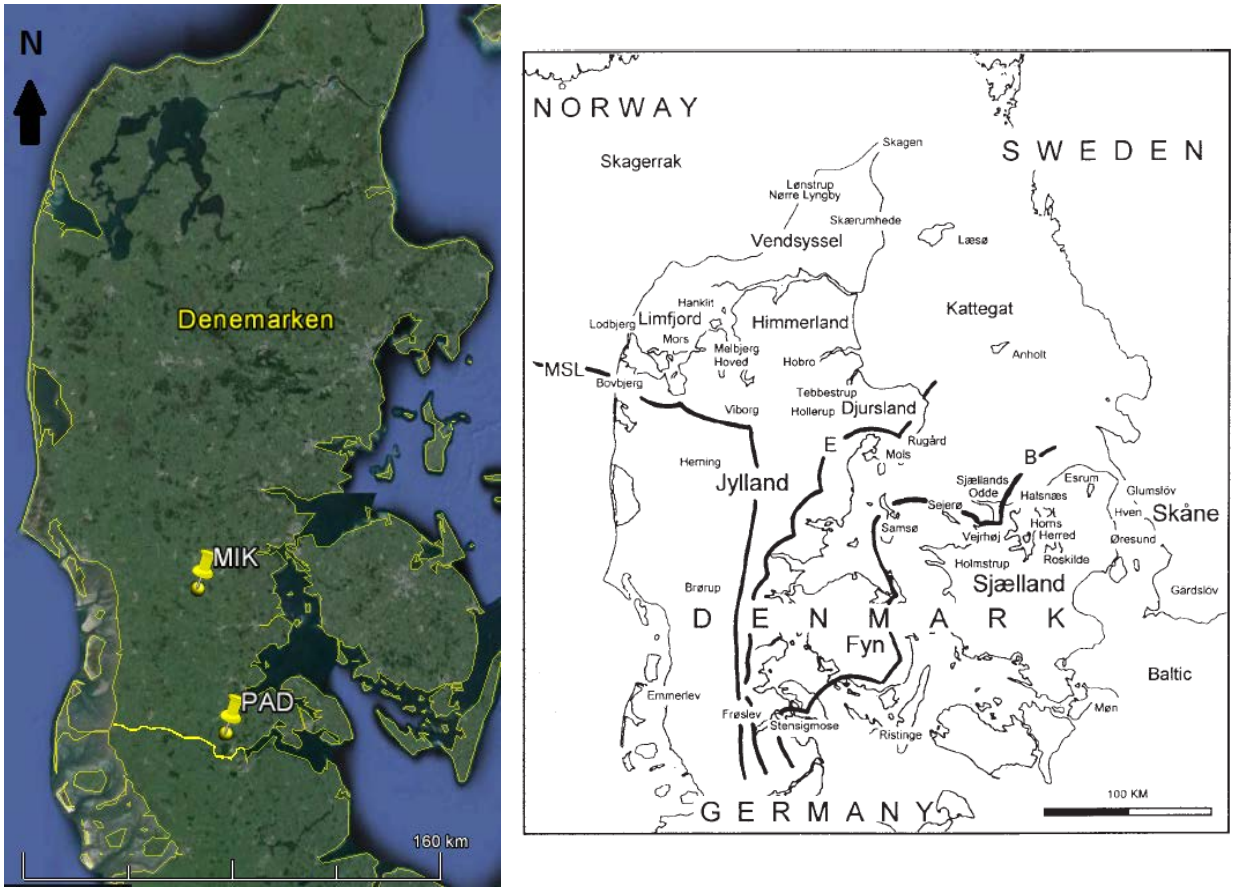

Figure 9: a) Fieldwork area Denmark, South Jutland, (Google Earth) b) Main Stationary Line (MSL) indicating the maximum extend of the Scandinavian Ice Sheet during the Weichselian, Houmark-Nielsen (1999).

Denmark is situated along the fringes of the Scandinavian ice-sheets, within reach of the glaciers that fluctuate in both growth and decay to both local and global (climate) dynamics (Houmark-Nielsen, 1999). The SIS spread out multiple times over the lowland of NW Europe during the Middle and Late Pleistocene (Houmark-Nielsen, 2007). During the Last Glacial Maximum (LGM) sequence (30-20 kyr BP) glaciers grew in the Scandinavian mountains in Norway and Sweden, causing southward advancement. This eventually led to the development of an ice stream from Norway to the Kattegat Ice Lake floor, to Denmark (Houmark-Nielsen & Kjaer, 2003).

The Late Saalien and Weichselian stratigraphy in Southern Jutland consists of a variety of periglacial and proglacial sediment. This indicates a periglacial landscape in Southern Jutland west of the Main Stationary Line (Houmark-Nielsen, 2007).

5. Methods

This chapter will describe the different methods used during the research. It is separated into three different parts; fieldwork methods, laboratory methods and an age model.

5.1 Fieldwork

5.1.1 Area selection

One general research area was selected for the Netherlands: the region around the Aekingerzand in northern Drenthe. This area was selected based on the numerous possible pingo remnants sites indicated by the geological and geomorphological maps of the area. Furthermore, these maps showed an influx of Late Medieval drift sand from the Aekingerzand area into the possible pingo remnants. This indicated a high potential for the preservation of the peat in the pingo remnant which, covered by drift sand, was likely protected from the peat digging of WWII.

Two research areas were selected in Denmark, one area based on its similarities to the Dutch fieldwork area, with Medieval drifts sands, close to the city of Ribe. The other selected area was approximately 5 km north of the German border (Ch. 3). Since Germany has pingo remnants within its borders (Bruijn, R. D., 2012; Ruiter, A. S., 2012), there is a high probability of pingo remnants close to the German border as well. The fieldwork in Denmark was planned in close cooperation with Dr. Aart Kroon, Copenhagen University.

5.1.2 Site selection

Pingo remnant selection took place during fieldwork preparation and during fieldwork itself. For site selection in the Netherlands, high resolution digital elevation maps from the Actueel Hoogtebestand Nederlands (AHN) and geological maps of the area were used. The maps were searched for circular depressions with a diameter of roughly 50-250 meters (Chapter 2). The selected sites were compared with Google Earth in order to determine if they were available for fieldwork. Afterwards, the sites were visited and their present characteristics were inspected on shape, topographic relief and proportions of present dimensions (tab. 2). If multiple of the characteristics from table 2 were recognized, a secondary inspection of the site took place by drilling.

The selection of sites in Denmark was done based on high resolution digital elevation maps (provided by Dr. Kroon, Google Earth and previously mentioned field observations.

5.1.3 Coring

If during field inspection a potential pingo site passed the first fieldwork inspection, a secondary inspection was performed in the form of a trial drilling. The drilling was done with an Edelman hand

corer, sometimes with a gauge attached to it, in the middle of the depression, since the most complete infill and climatological record is present there. However, due to a high water table, this was not always possible. When circumstances prohibited this, drilling was done as close as possible to the middle/deepest point in the depression.

If a site was chosen for further research after the initial drilling, and the circumstances allowed it, a transect was made to obtain a cross section. Depending on the diameter and infill of the pingo remnant, the average distance between the drillings would be 10-20 m. Cross sections were drawn for depressions with two or more drillings.

One of the depressions chosen for further analysis was partly filled up with water, resulting in drilling from a special uwitec drilling platform.

The sediment infills of the depressions were described directly in the field. The main focus was on finding lithological boundaries that could later be correlated with other cores in both the field and lab. The cores were also examined for the presence of calcium carbonate (CaCO3) with a 5% hydrogen chloride (HCl) solution. When present, the core was tested further in the laboratory.

Cores taken for further research in the laboratory were taken with the Piston corer. However, due to circumstances some cores were also taken with the gouge attached to the Edelman hand corer. All these cores were then placed into PVC-pipes, wrapped in plastic foils and placed into large plastic bags, before transporting them back to the laboratory for further research. When PVC-pipes were not available the cores were kept in the gouges and also wrapped in plastic foil.

5.1.4 Bathymetry

For the depression that was filled in with water, the bathymetry was measured using a Hand Held Sonar. The bathymetry was determined by dividing the lake into different sections and measuring the water depth in cross sections in each of those sections.

5.2 Laboratory methods

The cores were stored at 4-8 °C to minimize decomposing and degrading of the deposits in the cores. If applicable, the PVC-pipes were first cut in half, after which the cores were split with an iron wire. In case of very resistant peat, a sharp knife was used for the cutting. This splitting was done bottom up in order to avoid contamination from the younger sediments in the older sediments.

5.2.1 Lithological description

Lithological descriptions were done immediately after opening the cores in order to prevent discoloration of the deposits due to oxidation. A visual description was done of the coloration of the cores and samples were taken in order to determine the lithology of the deposits. Lithological boundaries were distinguished at sudden lithological and/or colour shifts or were approximated

where the lithological and/or colour shifts were more gradual. The resolution of the set boundaries is approximately 0.5 cm through the cores. This resolution could be lower in the upper parts of the cores, where there are young peat deposits rich in roots. During the lithological descriptions (sub)samples were taken for LOI and pollen.

5.2.2 Loss On Ignition

In order to determine the organic content of the cored deposits, the Loss On Ignition (LOI) method has been used (Heiri et al., 2001). Samples of approximately 1-2 cm^3 were taken with a sampling resolution of 1 cm throughout the cores and put into a crucible with a known weight. These samples were dried in a stove with a temperature of 105° C for approximately 12 hours in order to evaporate all the contained moisture. Afterwards, the samples were weighed and put into an oven with a temperature of 550° C for 4 hours, in order to burn the organics contained in the samples. After the samples had cooled below 100°C, but preferably still above 70°C, the samples were again weighed. The percentage of organic matter in the samples was determined using the following formula:

$$LOI(\%) = \frac{W_g - W_b}{W_d - W_b}$$

In which W_g stands for the weight of the crucible and the inorganic remains, W_b represents the weight of the crucible and W_d is the weight of the crucible and the moisture free sample (Heiri et al., 2001). Some of the inorganic remains were used for further analyses to determine the $CaCO_3$ content of the deposits that reacted to HCl in the field.

5.2.3 $CaCO_3$

The amount of $CaCO_3$ in the PAD core samples from Denmark was determined using a calcimeter based on Scheibler's method (Hoek and Bohncke, 2001). To determine the $CaCO_3$ with the calcimeter, the following basic chemical equation is used:

$$CaCO_3(s) + 2HCl(aq) \rightarrow CaCl_2(aq) + CO_2(g) + H_2O(l)$$

The inorganic remains that were left after burning for 4 hours at 550°C were used for further analysis. If $CaCO_3$ was present in these remains, CO_2 gas was released when a 5% HCl solution was added to this sample. This was then volumetrically measured by the calcimeter, which could then be used to calculate the fraction of $CaCO_3$ in the entire sample. However, first a calibration diagram was made to make it easier to calculate the amount of $CaCO_3$, which could then be divided by the total sample amount in order to get the $CaCO_3$ fraction.

5.2.4 Pollen analysis

Pollen samples were taken with a resolution of 5 cm. At an abrupt transition or possible hiatus, samples were taken just before and immediately after the disruption in the sediment. At more interesting lithological zones, with changing colours and different lithologies mixing, a higher resolution was applied of 2-3 cm. These pollen samples were prepared using the pollen preparation acetolysis protocol adaption after Feagri & Iversen (1964) of the Physical Geography Department at Utrecht University (Appendix 10.1, Dutch).

A pollensum of approximately 200 was counted for each depth. The pollensum only includes trees & shrubs, heather and upland herbs. The pollen counts were digitalized and made into pollen diagrams using the computer program TILIA (Grimm, 1992), where the exact pollen count for each depth is visible. A general lithology was also added to the pollen diagrams.

5.3 Age model

Based on the criteria from Hoek (1997) described in Chapter 3, Dutch pollen zones were identified and incorporated in the pollen diagrams. The pollen zones represent the general (Dutch) vegetation development during specific stadials and interstadials of the Lateglacial and Early Holocene, through which time can be linked to the derived results (Chapter 6). The Danish pollen zones are according to Hoek (1997), but agree with the pollen zones characteristic for specific time periods in Denmark Iversen (1973) and Mortensen et al. (2011). An LOI-based age interpretation of the infill was also made and is indicated on the LOI graphs (Chapter 6).

6. Results

6.1 Geomorphology and lithology

Each studied circular depression in this section will be described based on morphological characteristics and lithology, supported by a lithological cross section where possible. The Dutch coordinates are given according to the Rijksdriehoek (RD) coordinate system and the Danish coordinates are according to the Universal Transverse Mercator (UTM) coordinate system (tab. 5). Table 5 contains both the sites that were unusable for further research and the four sites selected for further research. The elevations in the Dutch Actueel Hoogtebestand Nederland (AHN) maps are given relative to the Nieuw Amsterdams Peil (NAP) and the elevations in the Danish Digital Elevations Maps (DEMs) are given relative to the Danish Vertical Reference 1990 (DVR90). The exception is the bathymetry map, the elevations in this map are relative to the water level in the depression itself.

Table 5: Drilled circular depressions with coordinates. Dutch depressions are given in RD coordinate system and the two Danish sites (bottom two in table) are given in UTM coordinate system. A small x marks absent coordinate data.

circular depression	x coordinates	y coordinates
1	219485	547242
2	219560	546860
3	219700	546902
4	219471	546770
5	217096	548556
6	216873	548293
7	217440	548512
8	217077	547810
9	216436	547183
10	213746	554186
11	214162	554477
12	215101	548852
13	217195	557075
14	217723	556829
15	217180	551490
16 (Groot Veen)	216275	547451
17	212796	547832
18	x	x
19	x	x
20	x	x
21	211939	546085
22	211848	546578
23	211865	546764
24	211887	546605
25	211352	546396
26 (Blauw Gat)	209137	542947
27 (MIK)	509459	6136451
28 (PAD)	519875	6882384

6.1.1 Blauw Gat, the Netherlands

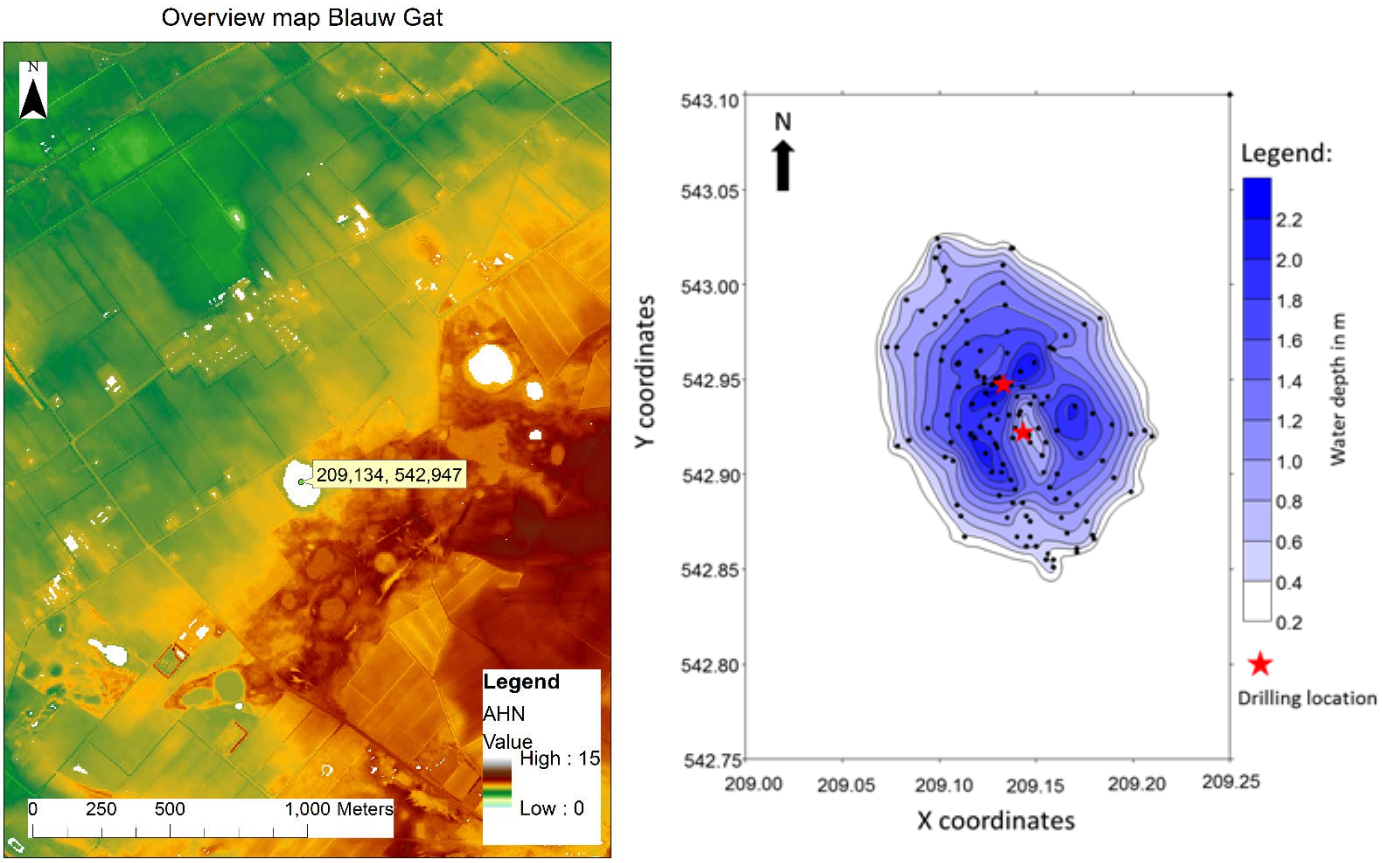

Figure 10: a) Actueel Hoogtebestand Nederland (AHN) map and b) bathemetric map Blauw Gat. Red stars indicate drilling locations.

The Blauw Gat depression (209.134; 542.947) is the local ice skating range of the village Vledderveen and is situated between different kinds of agriculture fields (fig. 10). The depression is now filled up with water and has a more oval than round shape. The dimensions of the depression are approximately 200 m in length and 130 m in width, with no surrounding rampart. The maximum water depth is approximately 2.40 m. Towards the center of the depression, the water depth slowly increases in all but for one area (fig. 10). According to old topographic maps of the area, peat was excavated in the depression accept for one small `island'. This small `island' is a logical explanation for the diverting topography. No outer rim was found surrounding the depression. Four cores were taken from two different drilling sites using the uwitec drilling platform.

A total of four cores were taken at the Blauw Gat depression in a N-S profile with the coordinates 209.134;542.947 and 209.143;542.922. Coordinates are noted above the cores to indicate that the visual representation of the taken cores do not follow the scale of the cross section (fig. 11). The specific names of the core parts are noted next to the parts.

The bottom of the infill of the circular depression is represented by fine sand at the bottom of the cores, after which deposition started in the depression. The infill of the depression seems to be similar at both coring sites, with at the base a sandy gyttja layer, followed by a small gyttja layer and thereafter peat. The peat layer is approximately 3 m thick and present all the way to the top of the infill. The composition of this peat layer changes throughout the infill; sand lenses and more sandy peat are also incorporated into the peat layer. The peat contains identifiable plant remains: an alternation of sedge and moss.

Clearly visible in the cross section is the ‘peat island’ sticking out above the other peat deposits, as noted on old topographic maps. Making this ‘peat island’ the spot with the most complete infill record.

Both the sandy gyttja and the gyttja layer are seen as the first infill in the pingo remnant after collapse, indicating the presence of a small lake during first infill of the pingo remnant. The peat indicates low water levels in the lake during deposition.

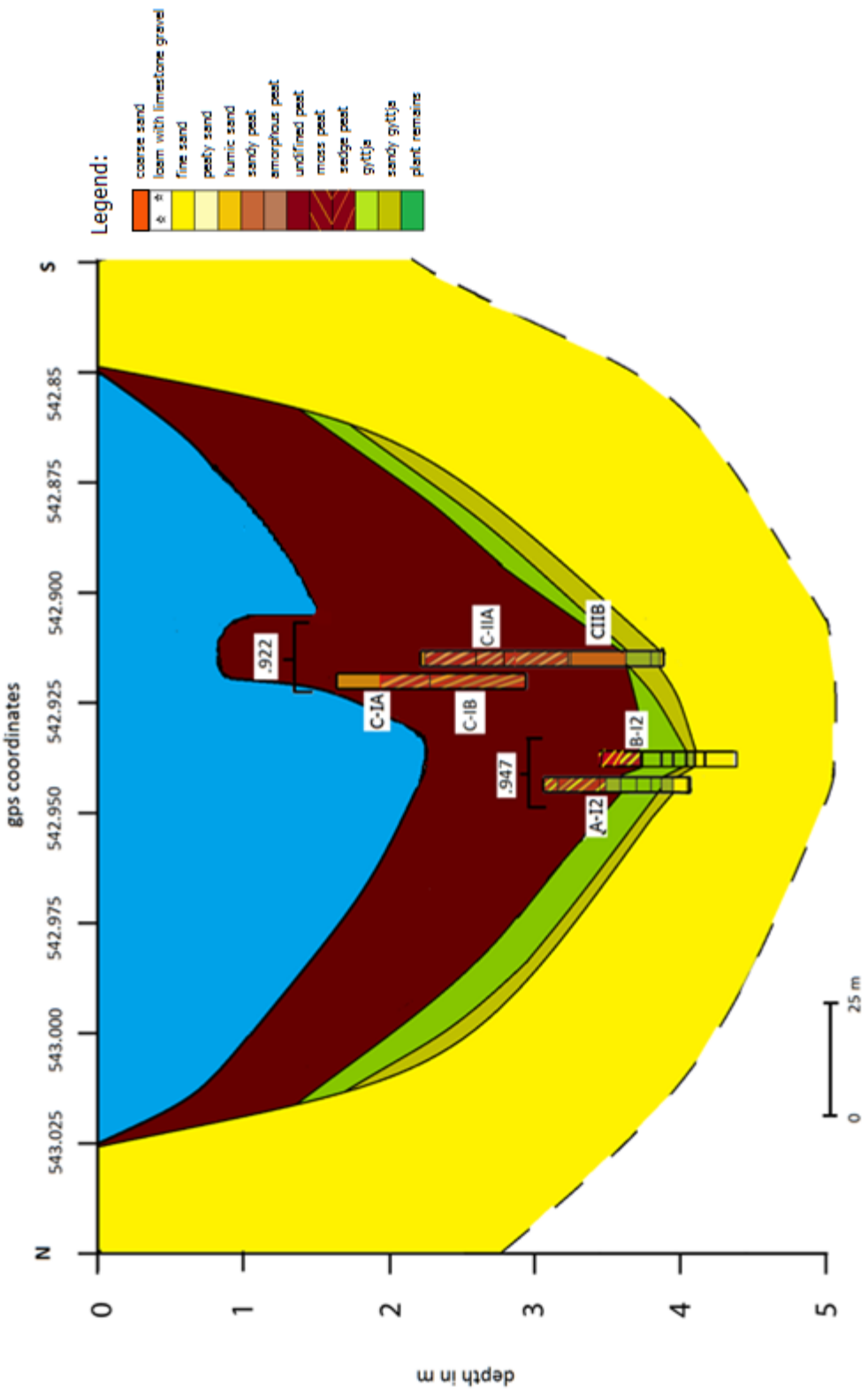

Figure 11: Lithological cross section Blauw Gat

6.1.2 Groot Veen, the Netherlands

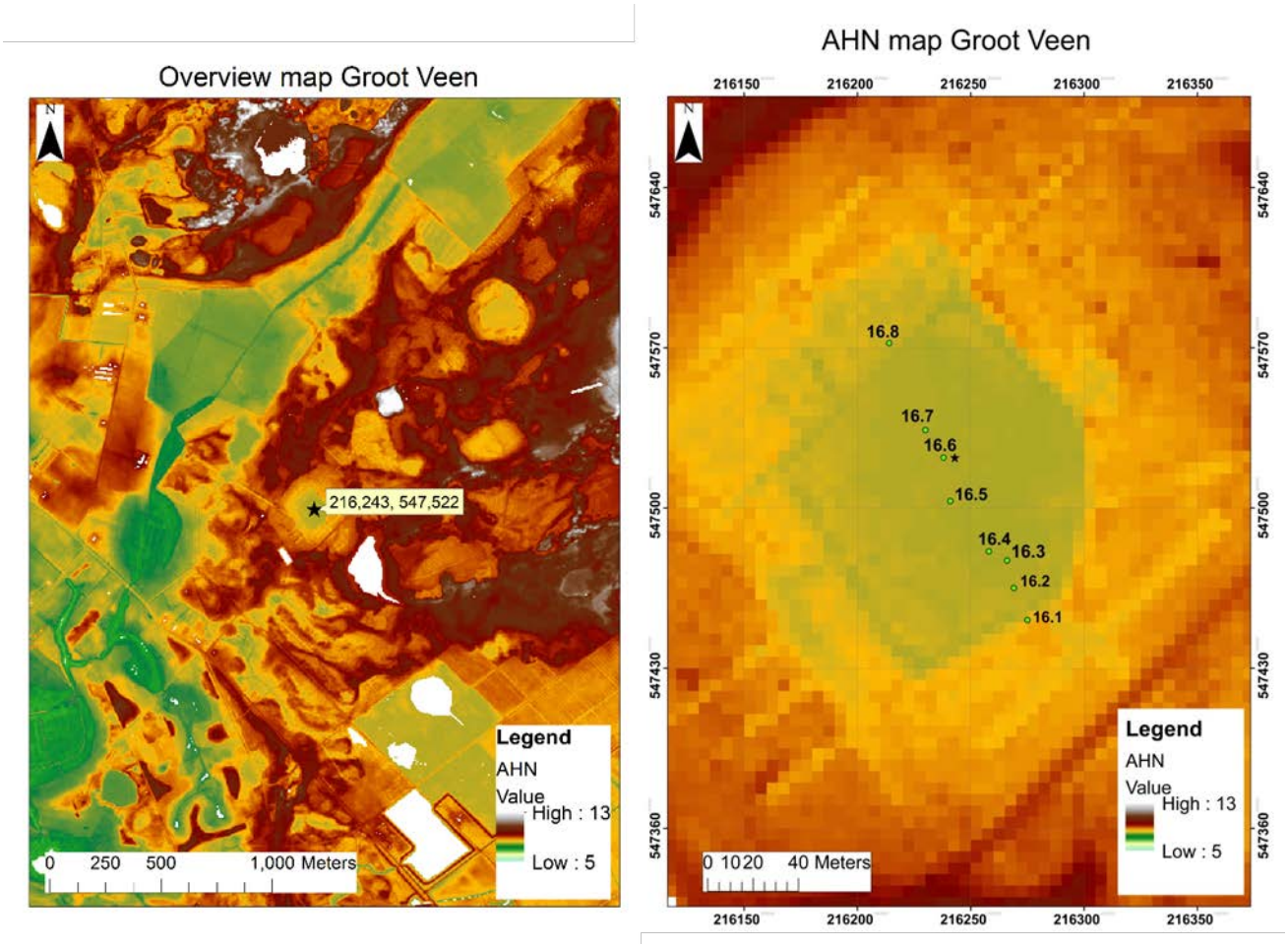

Figure 12: Actueel Hoogtebestand Nederland (AHN) of Groot Veen. Black star indicates sampling site.

The Groot Veen depression (216.243;547.522) is located approximately 2.5 km south-east of the village of Wateren and is situated within a woodland, surrounded by agricultural fields (fig. 12). The depression is a low lying well area during wetter periods. The shape of the depression is at present more square than round, indicating human interference and possible digging. According to the locals, peat has been excavated at the site, which might explain the shape. The depression has a diameter of approximately 135 m. Very little height difference is present in the depression itself, which again can be explained by human interference. No surrounding rampart was found.

A total of eight cores were taken at the Groot Veen depression in a N-S profile. The coring numbers (fig. 12) are noted above each core in the cross section (fig. 13).

The infill starts at the bottom of the circular depression, after the fine sand deposits, and seems to be comparable throughout the cores. The infill starts with either very small plant remains/peaty layer or a sandy gyttja layer, followed by a gyttja layer. A big layer of peaty sand and

sandy peat fills up the depression to the surface, for approximately 2 m. The last part of this layer was mostly very loose, not consolidated (fresh) peat.

These layers are seen as the filling up of a lake with deeper water conditions present at the start of the pingo infill with gyttja, followed by a shallowing of the lake with peat growth, which gradually filled up the lake. Plant remains were found at the start of the infill of the pingo remnant, which could have been organic matter that was present on the pingo remnant before collapse.

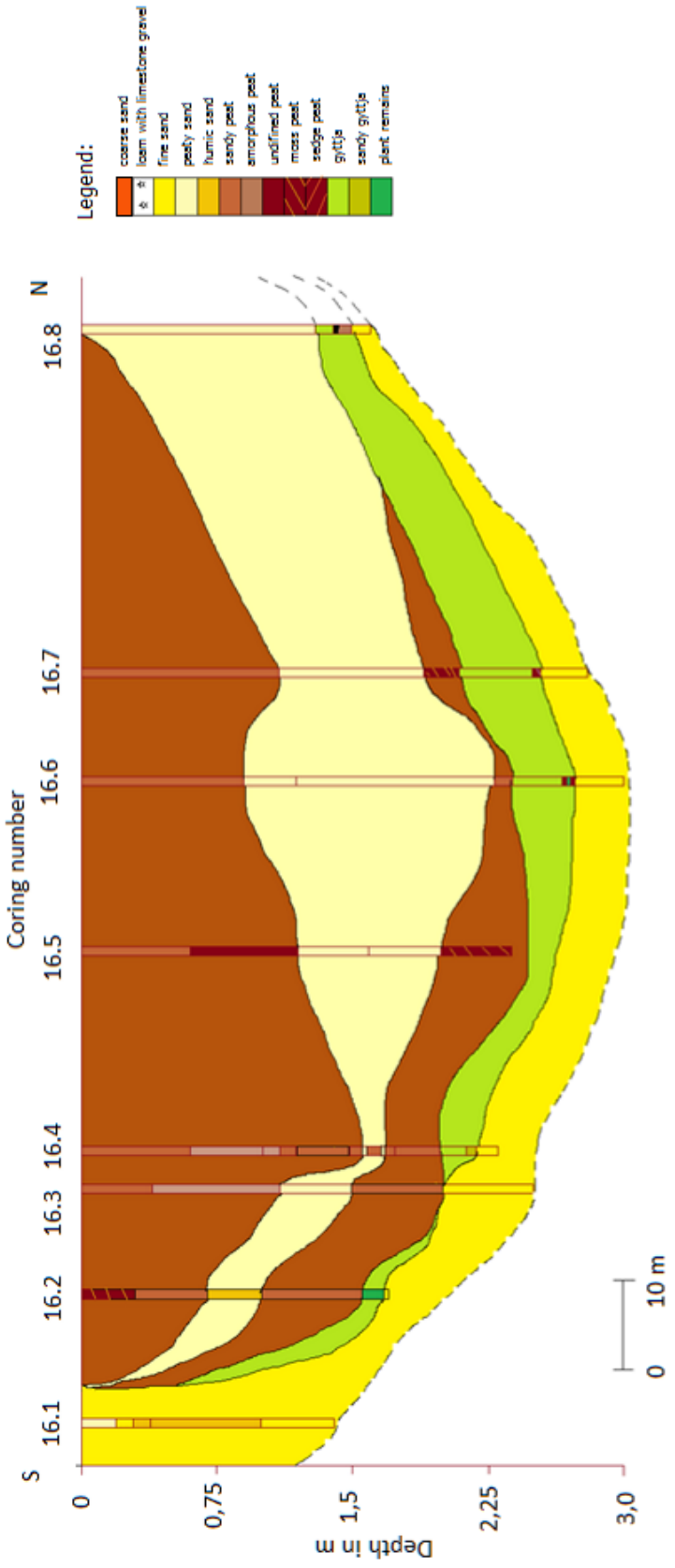

Figure 13: Lithological cross section Groot Veen

6.1.3 MIK, Denmark

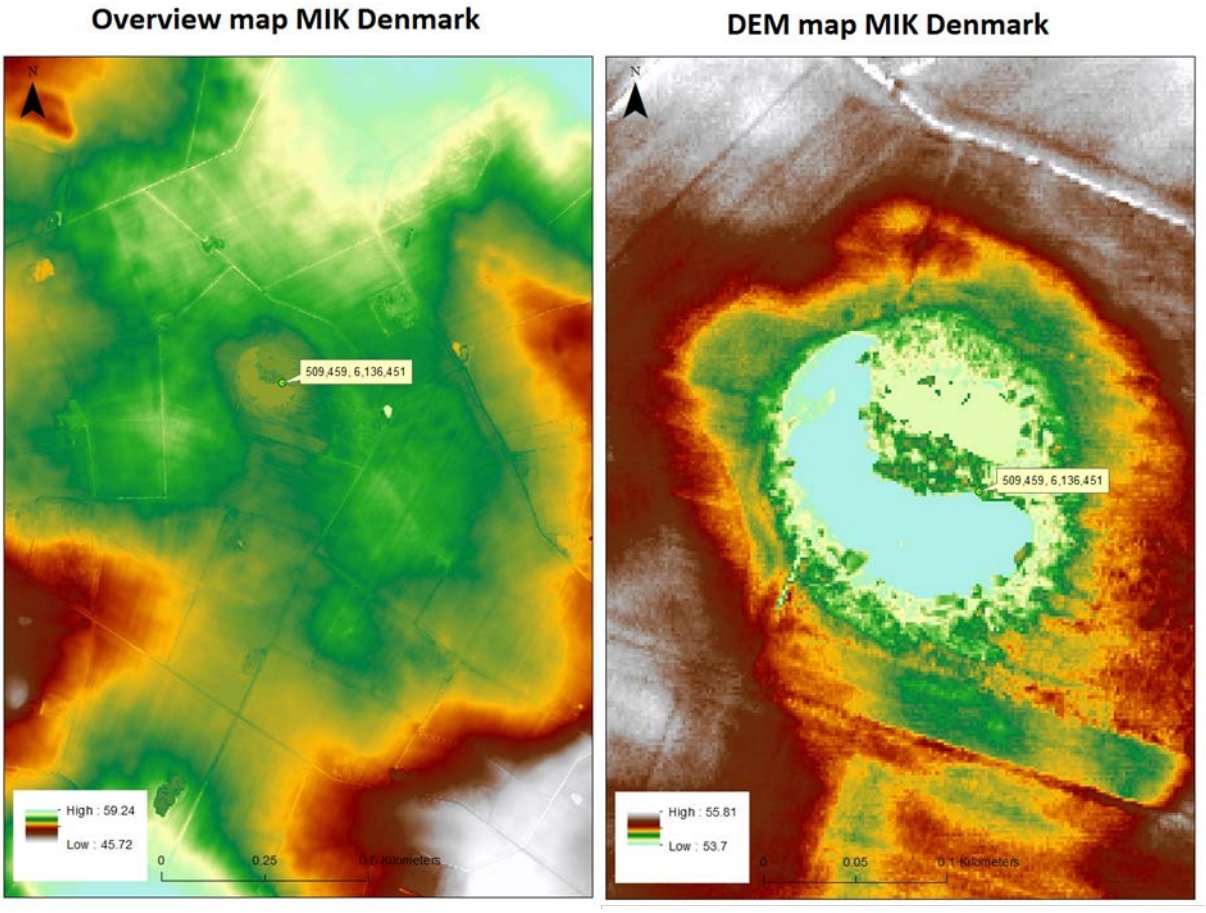

Figure 14: Digital Elevation Maps (DEM) of the MIK, Mette Bendixen, University of Copenhagen

The MIK depression (fig. 14), named after the village Mikkelborg, is located in the northern part of South Jutland (509.459;6.136.451) and is positioned between different agriculture fields. The depression is at present filled up with water, except for the north-east quarter of the depression, which is dry land and has a slightly higher elevation than the rest of the depression. The shape of the depression is almost perfectly round with a diameter of 150 m. There is very little height difference between the depression and its surroundings, making the depression not clearly recognizable on a DEM, but visible through its perfect round shape. Drilling was performed at the edge of the land in the depression and the water. No rim was found surrounding the depression.

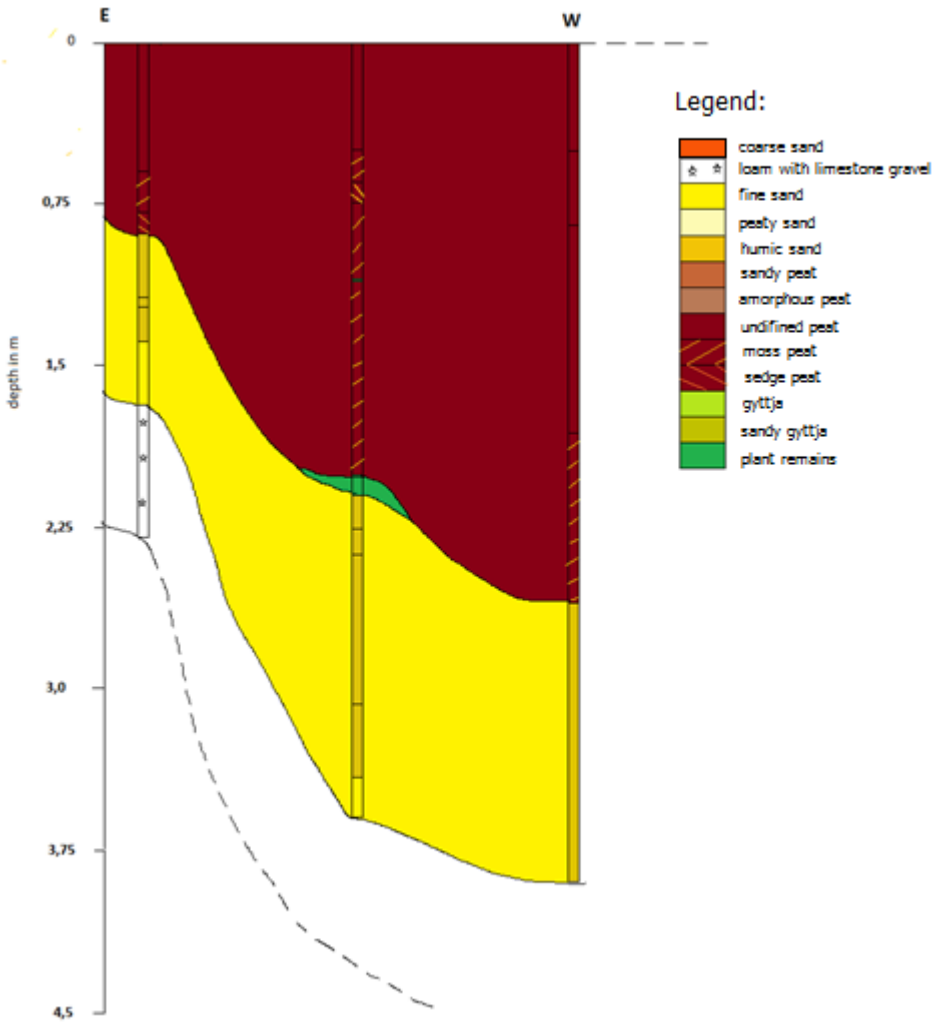

Figure 15: Lithological cross section MIK

A total of three cores were taken at the MIK depression in a E-W profile (fig. 15). Due to lack of GPS accuracy, no specific coordinates are available for the cores. The distance between the cores is approximately 15 m.

The infill seems to be comparable throughout the cores. The base of the infilling consists of loam with limestone gravel, followed by approximately 1 m of sand and 1.5 m of peat. The peat is mostly moss peat for approximately 1 m, after which it becomes amorphous. The upper part of the peat was mostly very loose, not consolidated (fresh) peat. Plant remains were found between the loam and peat in one core.

Due to the loam with limestones, easy penetrable sand and lack of gyttja it appears that this is a dead-ice hollow/filled up kettle hole (Chapter 2) with a diamict drape.

6.1.4 PAD, Denmark

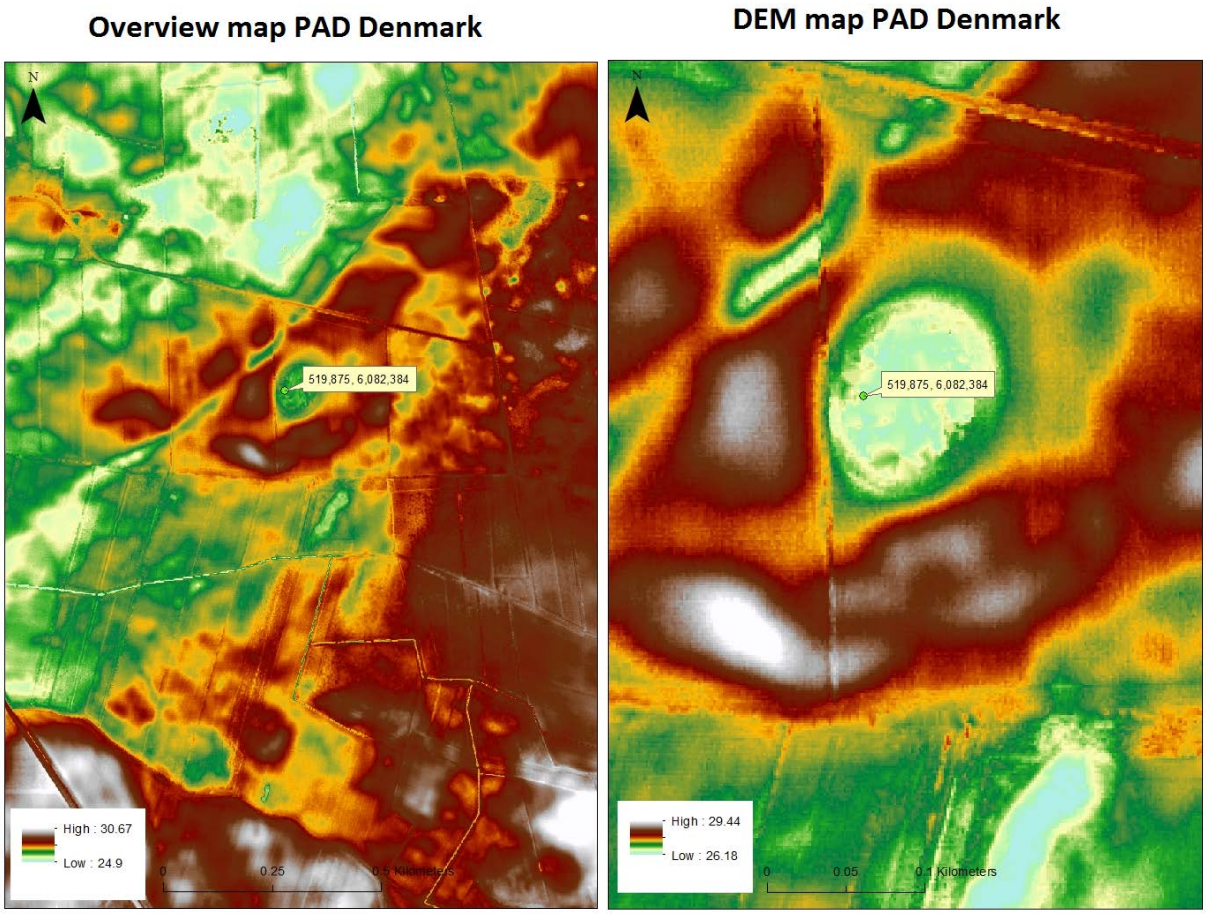

Figure 16: Digital Elevation Maps (DEM) of the MIK, source Mette Bendixen, University of Copenhagen

The PAD depression (519.875;6.082.384) is named after the local village Padborg, located in the south of South Jutland, approximately 10 km from the German border. The depression is situated in the middle of agriculture fields (fig. 16) with some trees surrounding it and is filled up with sediment to the surface. Although the DEM shows little height variation, the somewhat oval shape of the depression was easily recognizable. The dimensions of the depression are approximately 130 m in length by 100 m in width. No rim was found in the surrounding area.

A very small cross section (fig. 17) was made of the PAD depression, consisting of two cores, with a distance of approximately 10 m from each other (Appendix 10.2). The lithology of the deposits consists of half a centimeter coarse grey sand, followed by a very chalky gyttja layer, peaty gyttja layer and for the last approximately 2.5 m peat.

This infill has the same components and order as the lithology in the Dutch pingo remnants: sand bottom, gyttja layer base, followed by peat. This indicates that there was a lake with deeper water conditions present at the start of the pingo infill with gyttja deposits, followed by a shallowing of the

lake with peat growth, gradually filling up of the lake. Which makes it likely that this is in fact a pingo remnant.

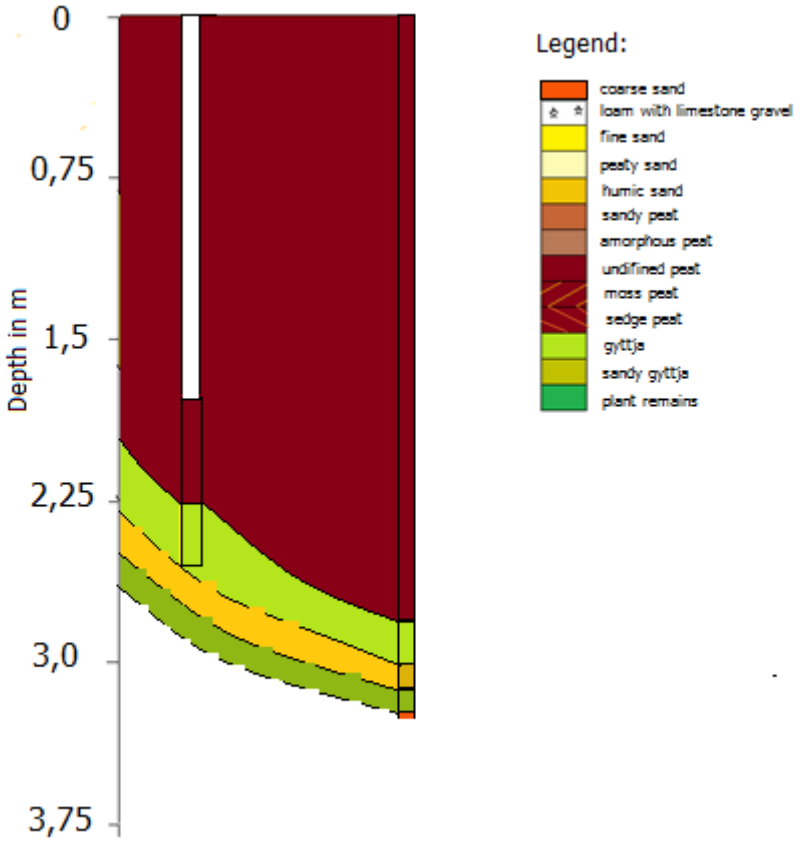

Figure 17: Cross section PAD depression

6.2 LOI results

The Loss On Ignition (LOI) has been determined on the cores from the selected four circular depressions. The LOI was measured from the bottom of each core up until far in the peat (Holocene). Only the lower parts of the LOI results are shown in this chapter, full details are in Appendix 10.3. An LOI-based age interpretation of the infill was made and is indicated on the graphs.

The organic portion of the material is dependent on both the influx of organic material and inorganic material. Since pingo remnants and most circular depressions have little fluvial input, the inorganic influx is assumed to be mostly from aeolian transport. Another minor contributor can be from chemical precipitation due to hydraulic seepage. The organic material in pingo remnants can both be from terrestrial and aquatic origins. The amount of organic material fluctuates due to multiple factors, such as local hydrology and topography. Moreover, formation and deposition of organic material is also assumed to be slower during colder and drier periods, and faster during warmer and wetter periods (Balyae and Clymo, 2001).

6.2.1 Blauw Gat, the Netherlands

The Blauw Gat LOI record (fig. 18) is divided into four intervals. The first boundary has been drawn just after the sand deposits end and the gyttja deposits start. The boundary has been set at 382 cm depth, at the rise of the graph towards higher organic values, from 5% to 25%. This interval has an average of 12% LOI, making it a zone with little organic material and high aeolian activity.

The following interval is from 382 cm to 358 cm. The boundary was put at the rise in organic matter content, which has an overall value of approximately 50% through the entire interval, until it dives below 25% at the next boundary. Overall a relatively smooth LOI curve in this interval, except for two small positive LOI peaks at 372 cm and 358 cm, indicating two small higher organic matter influxes.

The next interval is from 358 cm to 332.5 cm. The boundary for this zone was set at decreasing LOI values. It is characterized by low LOI values of on average 25%. The curve is still very smooth, except for one small maxima in LOI at 336 cm. This interval has less organic matter than the previous interval, but not as little as the first interval (~10%).

The last interval is marked by the rise of the LOI values at 332.5 cm. The organic matter increases from this point on until the organic fraction is almost 100%.

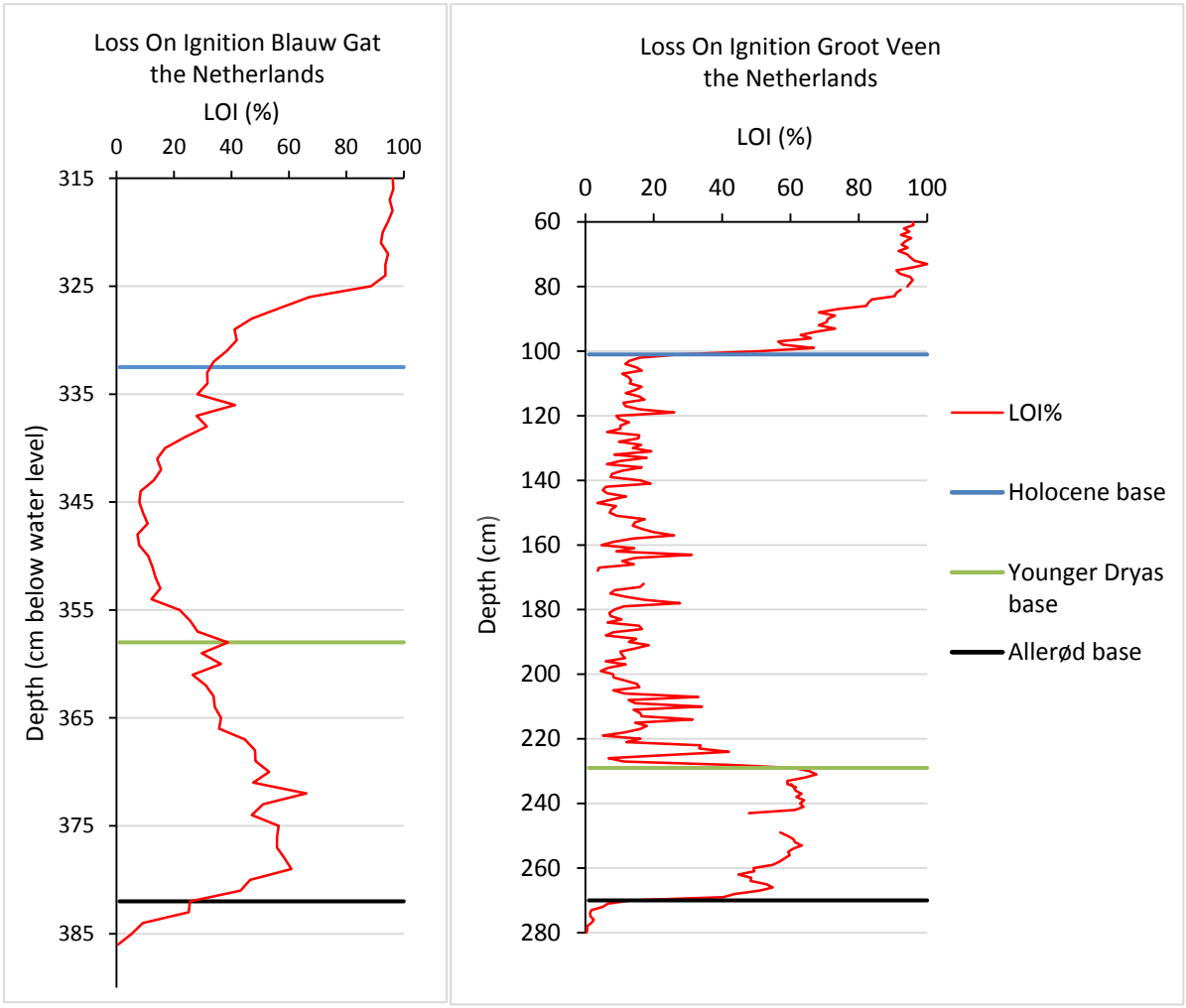

Figure 18: Loss On Ignition (LOI) Blauw Gat and Groot Veen

6.2.2 Groot Veen, the Netherlands

The Groot Veen curve (fig. 18) is also divided into four intervals. The first boundary has been drawn in the sand deposits, just before the gyttja deposits. The boundary has been set at 270 cm depth, at the very pronounced rise of the graph towards higher organic values, from almost 0% up to approximately 60%. This very small interval has an average of 1% LOI, making it a zone with almost no organic material.

The following interval is from 270 cm to 229 cm. The boundary was set at the sharp fall in organic material towards the following zone. This interval has a relatively high organic matter content of approximately 65%.

The next interval is from 229 cm to 101 cm. The boundary for this interval was set at very sharp, decreasing LOI values, characterized by LOI values of on average 15%. Moreover, the signal has a very saw-tooth like pattern in this interval. Some LOI maxima of ~30% are present at 214 cm and at 163 cm. This interval has less organic matter than the previous interval, but not as low as the first interval (~10%).

The last interval is marked at the sharp rise of LOI values at the end of the previous interval (101 cm). The organic influx increases from this point on to almost 100%.

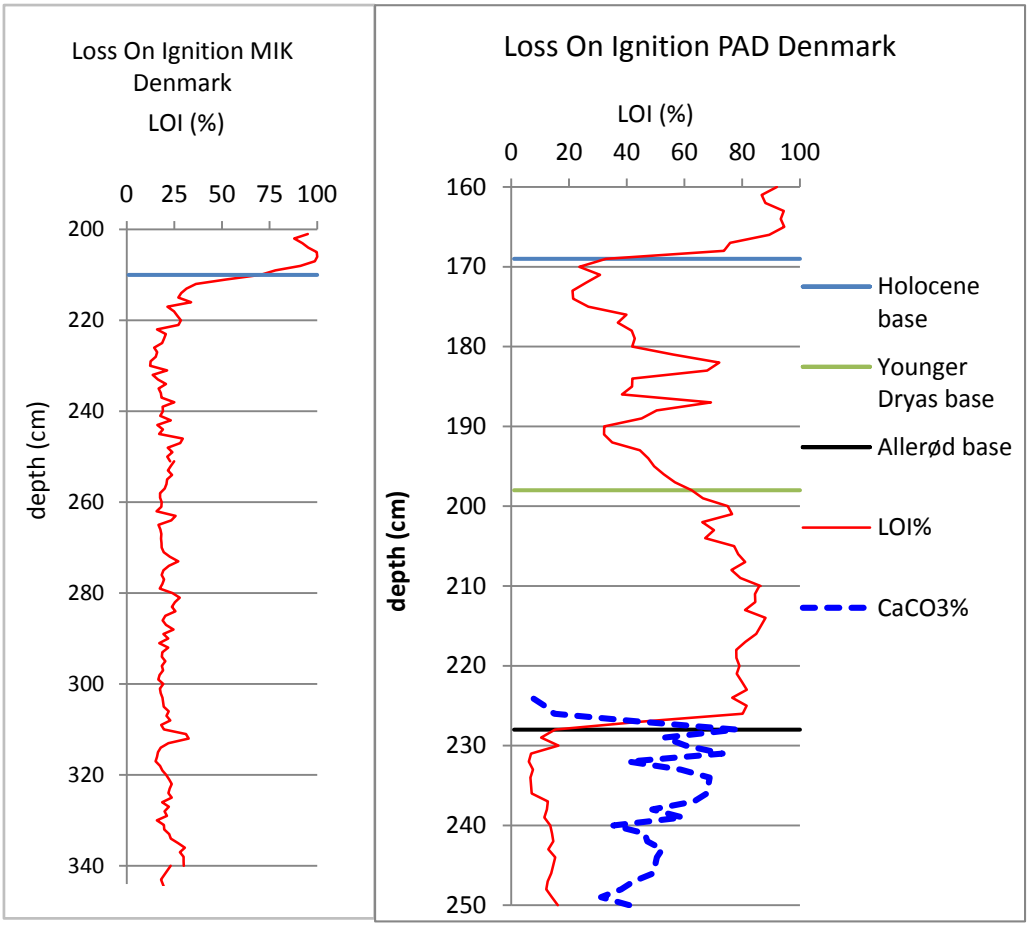

Figure 19: Loss On Ignition (LOI%) MIK and PAD

6.2.3 MIK, Denmark

Only one interval was determined in this graph (fig. 19), the boundary of the Holocene at 210 cm. The LOI signal from 340-210 cm is rather consistent with values of around 20% organic matter, up to a sharp rise at 210 cm to ~99% organic matter.

6.2.4 PAD, Denmark

The first interval in this graph (fig. 19) is from 250 cm to 228 cm. The interval is characterized by a very low organic matter content (~12%) and a very high $CaCO_3$ content (~65%).

The second interval in this graph is from 228-198 cm. The start of the interval is marked by a sharp transition towards a higher organic matter content of approximately 80%. These higher organic matter concentrations are consistend until a decreasing trend starts at 198 cm. Furthermore, a very small organic matter peak is present just before the end of the interval at 201 cm.

The following interval starts at 198 cm with slowly decreasing LOI values until a lower organic matter concentration of approximately 37% is reached, with two LOI maxima at 182 cm and 187 cm that have a LOI of ~70%. The interval ends when the LOI concentrations increase significantly at 169 cm, resulting in a sharp transition from lower to higher values.

The last interval starts with a sharp transition towards high LOI values of approximately 95%, which continue until the end of the LOI diagram.

6.2.5 Interpretation and preliminary conclusions Dutch sites

The LOI records of the Dutch depressions are similar, although more pronounced in the Groot Veen record. Both LOI records could be divided into four different zones, an interpretation of these zones is made from bottom to top.

The LOI record in the first zone indicates an open landscape where sediment is available for transport. For example a colder environment at the end of a glacial period.

The increase in organic matter in the second zone may indicate a warmer or wetter environment, with a significant aeolian influx. This indicates a warmer period in an overall cold environment, where there is denser vegetation and less opportunity for aeolian transport, this could be connected to the Allerød.

The third interval is interpreted as a cold/wet interval that is less cold/wet then the first interval, with a more open vegetation with more aeolian transport. Short warmer/wetter phases with slightly higher organic matter content occur as well during this interval. This makes the Younger Dryas a logical chronological zone for this interval.

The high amount of organic matter in zone 4 can only indicate very favourable conditions for vegetation growth during which the vegetation has closed up and aeolian transport was limited. This indicates a warmer period, possibly of Holocene age.

6.2.6 Interpretation and preliminary conclusions Danish sites

The LOI records of the Danish depressions are very different. Therefore, a separate interpretation will be given for each depression.

6.2.6.1 MIK

The low organic matter curve in the MIK depression can indicate a very long, cold, wet period. However, since this is very unlikely because of our known Quaternary history, it seems more logical that some form of disturbance has occurred at the bottom of the infilling of this circular depression. The high organic matter values up to almost the top of the infilling indicate a closed, warm vegetation cover. Therefore, the interpretation as Holocene has been given to the last ‘interval’ in this graph.

6.2.6.2 PAD

The first interval may indicate the end of a cold and wet period with barren vegetation and hydraulic seepage that is becoming warmer and drier in which calcium carbonate can precipitate. The chronological time period connected to this interval is could be the last part of the Older Dryas, transitioning into the Allerød or the start of the Allerød in which organic matter is still low.

The second interval has significantly more organic matter than the previous interval, indicating a more closed vegetation cover, in a warmer/wetter climate with less loose sediment available for transport. These characteristics are used to interpret the chronological time zone as being the Allerød.

The lower LOI values indicate a colder climate, with a more open vegetation than the previous interval, but more closed and warmer than the first interval. Therefore, this interval is considered to be deposited during the Younger Dryas.

The very high concentration of organic matter indicates a very favourable environment for vegetation growth, with a dense vegetation in which barely any sediment can be transported by aeolian activity. All these factors indicate a Holocene age for this interval.

6.3 Pollen results

The pollen diagrams are based on an average of 20 subsequent depth samples. Due to low pollen concentrations, multiple slides were sometimes counted in order to achieve a reliable pollen count of approximately 150-200 pollen. A simplified lithology has been added to each pollen diagram. Longitudinal bars were added to the graphs for an exaggeration of the results to make them easier to interpret. Different vegetation zones are determined based on Chapter 3 (Hoek, 1997; Geel et al, 1989).

6.3.1 Pollen diagram Blauw Gat, the Netherlands

Pollen zone 1 could not be divided into different subzones, the entire zone is determined to be from 386-380 cm. Zone 1 is characterized by an increase in *Betula* pollen percentages and increasing AP percentages (fig. 20). Many pioneer species are present (*Artemisia*, *Plantago*, Poaceae, *Koenigia islandica*), but with decreasing percentages throughout zone 1. They represent a vegetation where arctic elements (*Koenigia islandica*) are present. The local environment appears to be wet, with relatively high amounts of different aquatic vascular plants, although not in high percentages. Algae are also present in high percentages.

Pollen zone 2 can be divided into two different subzones in this diagram: 2a and 2b. Subzone 2a is present from 380-370 cm. Subzone 2a is here characterized by high values of *Betula* pollen percentages, low *Salix* pollen percentages and an overall rise in AP and decrease in NAP. The contribution of tree species is approximately 85% and the contribution of upland herbs has gone down to approximately 15%. New upland herbs are introduced (Amaranthaceae, *Helianthemum*, *Polygonum,* Ranunculaceae, *Filipendula*), which is indicative of pioneer species in this zone (van Geel, 1988). Pollen subzone 2b is present from 370-362 cm. This subzone is characterized by an increase in *Pinus* pollen percentages. AP percentages are still increasing, while NAP percentages are decreasing. Heather is present in small percentages. The local environment changes as aquatic (Sphagnum) percentages increase and Pediastrum and Botryococcus (Algae) percentages decrease. Subzone 2b represents a developing vegetation with pine forests.

Zone 3 is divided into two different parts: 3a and 3b. According to Chapter 3 subzone 3a (362-350 cm) is characterized by decreasing *Pinus* and *Betula* pollen percentages. However, in this case only *Pinus* pollen percentages decrease. The AP percentages decrease slightly and NAP percentages increase slightly. Most of the upland herbs present in zone 2 are no longer present in subzone 3a. Subzone 3b (350-339 cm) is characterized by a rise in *Empetrum* pollen percentages. The NAP percentages increase while the AP percentages decrease. The local environment changes as aquatics percentages decrease (Sphagnum) and algae percentages increase (Botryococcus).

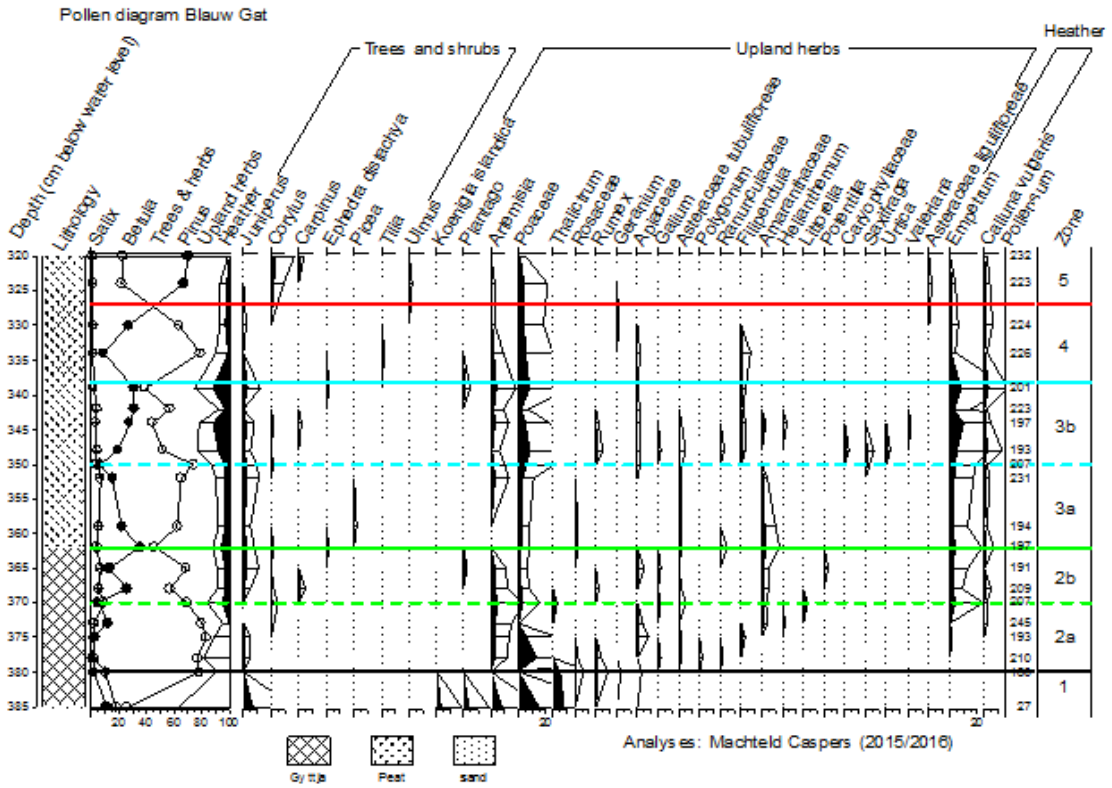

Figure 20: Pollen diagram Blauw Gat

Pollen zone 4 is present at 338-327 cm. It could not be subdivided, and is marked by an increase in *Betula* pollen percentages and an increase in AP percentages throughout the zone. There is very little variety in the upland herbs present in zone 4 (*Artemisia*, Poaceae*, Geranium*, *Filipendula*, Asteraceae liguliflorae)

Pollen zone 5 starts at 327 cm and continues until the end of the pollen diagram. Zone 5 is characterized by increasing *Pinus* pollen percentages. *Betula* pollen percentages decrease and *Corylus* pollen slightly increase.

6.3.2 Pollen diagram Groot Veen, the Netherlands

The Groot Veen depression has been investigated before by the Rijks Geologische Dienst (RGD) (Ter Wee, 1966). A small comparison shall be made between both pollen diagrams (Appendix 10.4) after the Groot Veen pollen diagram has been described and divided into different vegetation zones after Hoek (1997).

6.3.2.1 Description

Pollen zone 1 is present in the Groot Veen record (fig. 21) at 267-250 cm and can be subdivided into subzones 1a, 1b and 1c. In this pollen diagram only the subzones 1b and 1c are present. The

boundaries for subzone 1b are set between 267-265 cm. It is characterized by relatively high *Betula* pollen percentages and AP percentages. Many different upland herbs (Poaceae*, Apiaceae, Rumex,* Rosaceae*, Thalictrum, Galium, Artemisia*) are present in small percentages and continue into subzone 1c. Subzone 1c starts at decreasing *Betula* pollen percentages, increasing *Salix* pollen percentages and at the lithological transition from sand to gyttja. There are high percentages of fern (*Equisetum*) pollen and aquatic vascular plants (Cyperaceae and *Menyathes trifoliate*), indicating a local wet environment.

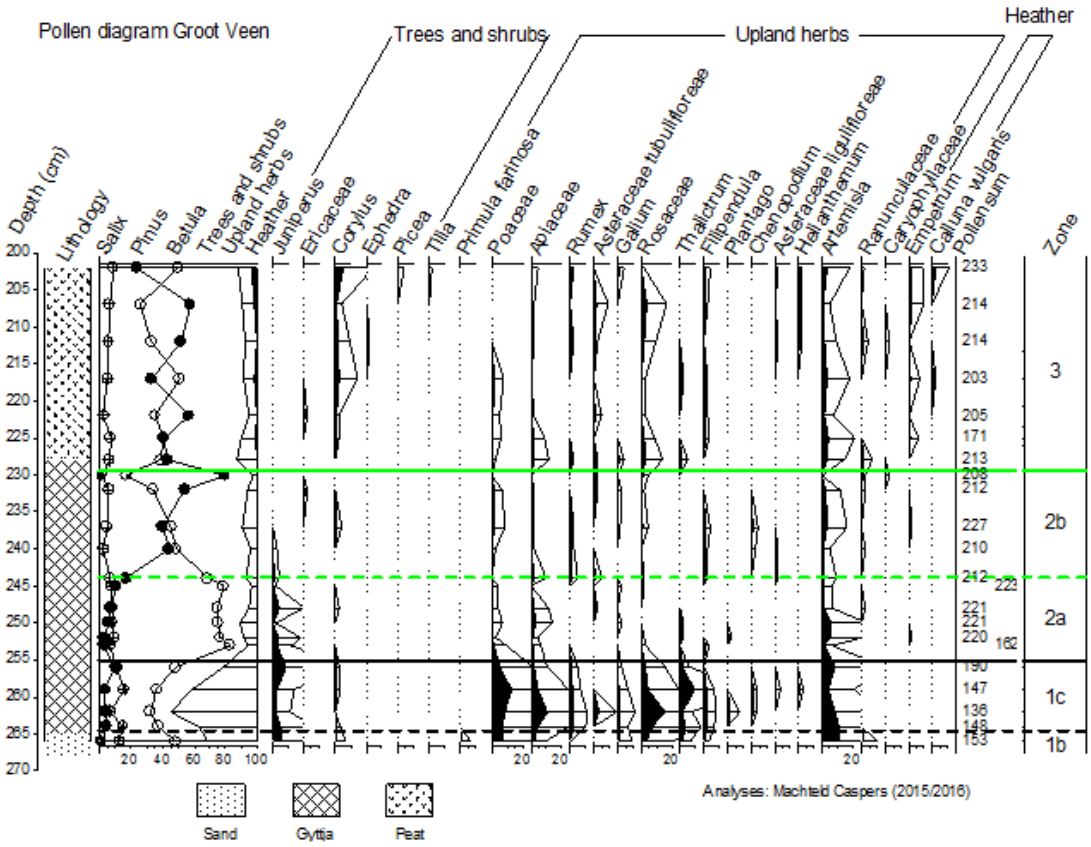

Figure 21: Pollen diagram Groot Veen

Pollen zone 2 is present in the Groot Veen pollen diagram (255-229.5 cm), it has been subdivided into subzones 2a and 2b. Subzone 2a (255-244 cm) is characterized by sharply increasing *Betula* pollen percentages and declining *Salix* pollen percentages. There is a steep decline in NAP percentages, many of the upland herbs still present in zone 1c stop occurring in this zone. The local environment is very dry, and barely any aquatics are present. Subzone 2b (244-229.5 cm) is characterized by a large increase in *Pinus* pollen percentages. The *Betula* pollen percentages decline in this subzone. Furthermore, there is a very small increase in the upland herb percentages and a slight increase in the amount of aquatic species.

Pollen zone 3 is here characterized by a decline in *Pinus* pollen percentages and an increase in *Betula* pollen percentages. The percentages of both *Pinus* and *Betula* fluctuate slightly through zone three (5-10%), but their percentages are on average equal to the other. Most of the upland herbs present in subzone 2b are present in zone 3 as well. Moreover, the contribution of heather is visible for the first time, both *Empetrum* and *Calluna* are present. The occurrence of *Empetrum* is characteristic for the northern part of the Netherlands for subzone 3b (Hoek 1997). This might indicate that zone 3b starts around 207 cm, where a slight increase in *Empetrum* is observed, but this is not conclusive. Zone 3 has a slightly higher amount of aquatic plants than zone 2.

6.3.2.2 Comparison

Both pollen diagrams are very similar, bearing in mind that the pollen diagram from 1966 follows a different grouping system with a different pollensum, resulting in different pollen percentages. The base of the Groot Veen diagram in this research is easy to correlate with the diagram from the RGD (Appendix 10.4). At the base of the Groot Veen diagram a large amount of Equisetum is present, which is also present approximately 15 cm above the base in the RGD diagram. Moreover, both diagrams show a relatively high percentages of upland herbs and *Betula* pollen at the base. Similar trends can be observed in the pollen diagrams in the tree pollen percentages and in the upland herbs percentages from the base upwards.

6.3.3 Pollen diagram MIK, Denmark

Three slightly different Dutch vegetation 'zones' could be defined in the Danish MIK pollen diagram (fig. 22). The two basal pollen zones (345-331 cm and 331-308 cm) do not have any major pollen changes. Only very small changes occur in the pollen spectra; a very small increase in *Betula* pollen percentages at the base of the pollen diagram led to categorizing the basal zone as Dutch vegetation zone 2 and a small decrease in *Pinus* pollen percentages at the border for the next zone led to a categorization of zone 3. These very small changes could be considered insignificant, therefore question marks are raised about assigning Dutch vegetation zones 2 and 3 to these pollen zones. The pollen that were found and identified in these 'zones' were often very lightly colored and badly damaged. The only zone that was defined with some certainty was zone 4. This zone was marked by a very slight increase of *Betula,* a marker for the onset of the Holocene (Hoek, 1997; Iversen, 1973; Mortensen et al, 2011).

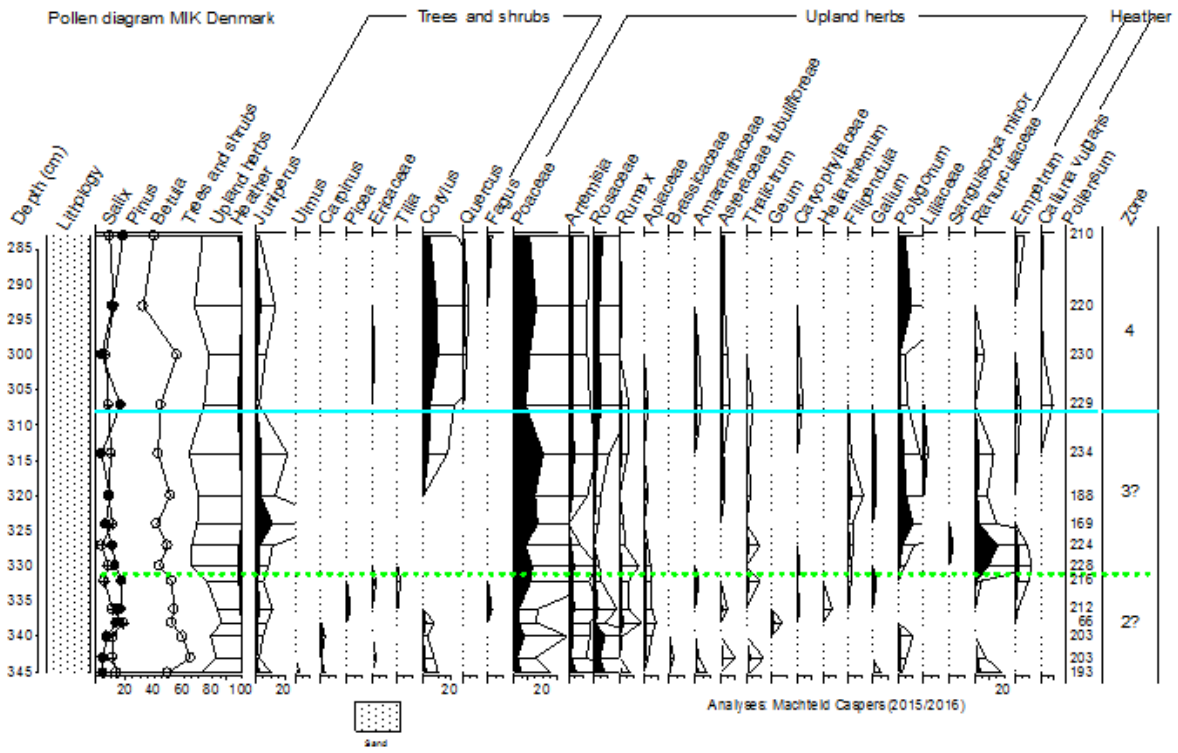

Figure 22: pollen diagram MIK Denmark

6.3.4 Pollen diagram PAD Denmark

Pollen subzone 1b is present from 250-246 cm. It is characterized by abundant (~40%) and increasing percentages in *Betula* pollen (fig. 23). Furthermore, high percentages of Poaceae (20%) and *Artemisia* (20%) pollen are present, although declining throughout the subzone. Pollen subzone 1c is present from 246-239 cm and is characterized by decreasing *Betula* pollen percentages, slightly increasing *Salix* pollen percentages and an increase in the NAP percentages. Poaceae pollen percentages increase simultaneously with the decrease of *Betula* pollen percentages.

Pollen zone 2 is present from 239-230 cm and is marked by a large increase in *Betula* pollen percentages. *Artemisia*, Poaceae and general upland herbs percentages decrease. Overall, the vegetation is becoming denser, which is according to Hoek (1997) characteristic of zone 2.

Pollen zone 3 starts at 230 cm and continues until the end of the pollen diagram. This zone is marked by decreasing *Pinus* pollen percentages. However, the *Betula* pollen percentages are also supposed to decrease according to Chapter 3, but the percentages increase.

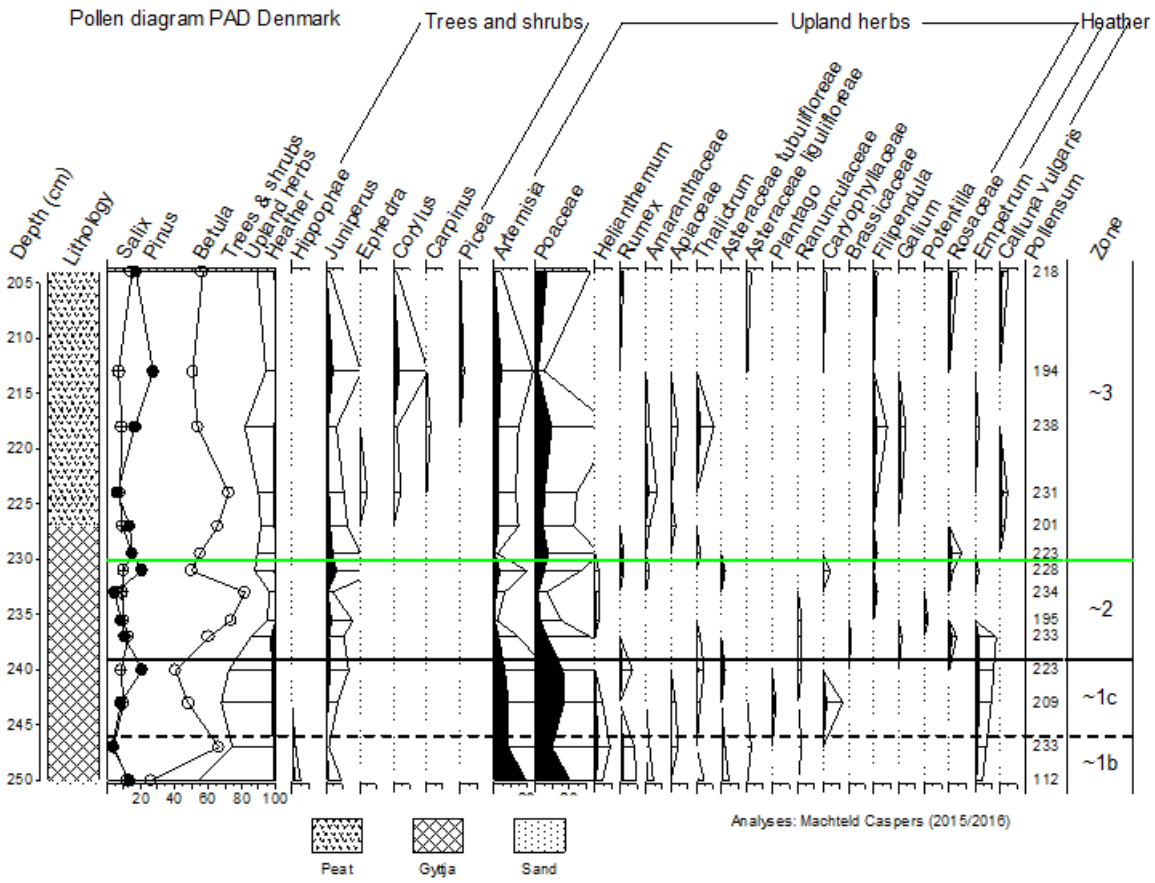

Figure 23: Pollen diagram PAD Denmark

6.3.5 Interpretation and preliminary conclusions Dutch pollen spectra

These pollen spectra are similar and could be categorized according to Chapter 3. Therefore, a short vegetation interpretation for both Dutch sites is given here.

Pollen zone 1 has been defined by van Geel et al. (1989) and Hoek (1997) as having a relatively low percentage of arboreal pollen and high percentage of upland herbs of which some prefer artic conditions. It shows the development of herbaceous plant communities and small shrubs due to increasing temperatures in a still cold environment (Hoek, 1997). They represent the pioneer species in an open landscape. Pollen zone 2 shows the further development of the vegetation into an open birch forest and later a pine forest during the warmer Allerød interstadial (Hoek, 1997). Pollen zone 3 is a perfect example of a denser vegetation that is being halted in a colder stadial (Younger Dryas) while herbaceous communities develop (Hoek, 1997). At the beginning of zone 4, which can be considered equivalent to the Preboreal interstadial, the birch forests expands, marking the onset of the Holocene.

6.3.6 Interpretation preliminary conclusions Danish pollen spectra

The Danish pollen spectra are very different. Therefore, a short separate vegetation interpretation will be given.

Although Dutch vegetation zones 2 and 3 were applied on the MIK pollen diagram, the characteristic pollen zone changes were barely or, one could argue not, present. Moreover, no overall changes occurred in the pollen spectrum. Therefore, no vegetation development can be described for this part of the pollen diagram. The upper part of the pollen diagram, categorized as zone 4, did have the characteristic rise in *Betula* pollen percentages. However, very few other changes occurred in the pollen spectrum. No vegetation development can be derived from this graph.

The PAD pollen diagram is very similar to the Dutch diagrams. The same vegetation development can be applied, with some small differences. Iversen (1973) describes *Betula* pubescens as a marker for the Bølling, the bottom part of the pollen diagram, subzone 1b. The vegetation during this interstadial is described as 'park tundra', with birch wood in the warmer places and tundra in the colder, damp areas (Iversen, 1973; Mortensen, 2011)). The following subzone 1c is considered to be equivalent to the Older Dryas stadial (Hoek, 1997). The period is seen as a deterioration of the climate (Iversen, 1973) in which trees decreased and upland herbs increased for a few centuries. Zone 2 indicates a vegetation with *"climatic improvement*" (Iversen, 1973), represented by dominating birch forests during the whole Allerød. Pine can occur sparsely as well during this period (Iversen, 1973; Mortensen, 2011). The last zone 3, is characterized by a vegetation that changed due to sudden temperature decrease; open part tundra replaced most of the vegetation in Denmark (Iversen, 1973).

7. Discussion

7.1 Geomorphology

Although pingo remnants are considered to be circular depressions, their shape does not have to be perfectly circular, oval shapes are common as well, and ramparts can also be present (Mackay, 1998).

The two Dutch reference pingo remnants do not have a round shape or raised rim around the depressions. The Blauw Gat pingo remnant is oval shaped, while the Groot Veen pingo remnant is neither oval or round (related to peat digging).

The MIK depression is the most round of all four depressions, on first sight it even appears to be almost perfect circular. The PAD depression is very similar to the Blauw Gat pingo remnant, very oval in shape. Both Danish depression do not have raised rims.

While looking at the geomorphology of these features, human influence should be taken into account. All the remnants are located in agricultural areas, where farmers flatten the surface for agriculture, which would explain the absence of rims at all the different sites.

7.2 Lithology

The Blauw Gat and Groot Veen pingo remnant are very similar in their lithology as can be seen in the cross sections. Both have the distinct sandy basal fill, followed by a couple of decimeters of gyttja, followed by different kinds of peat infilling. However, the Groot Veen pingo had some extra features; plant remains at the base of the infill, just above the sand, and a distinct sandy peat layer within the peat. It appears that when the pingo collapsed, the vegetation cover on top of the pingo came down with it and part of it was preserved at the bottom of the newly arisen lake. The thick sandy peat layer shows that more aeolian transport and deposition was taking place around the Groot Veen depression compared to the Blauw Gat pingo, which could be related to the smaller distance to many cover sand deposits in Drenthe.

The MIK depression has a very different lithology than the Dutch pingo remnants. One of the main differences was the large sand layer, through which could be drilled and the loam layer with small limestone gravel was reached. Loam and gravel are not characteristics that belong with pingo remnants, but go with glacial till (Ben & Evans, 2011). Taking this into account and looking at the alternative explanations for circular depressions, a kettle hole/dead ice hollow does not seem an unlikely explanation for this depression. The MIK depression is located closed to the previous Main Stationary Line, which makes the idea of a dead ice hollows that was created when an isolated block of ice from the ice sheet melt-out was buried, seem very likely. This can be the case when the infill of these depressions have a thick diamiction layer.

The lithology of the small PAD cross section is very similar to those of the Dutch pingo remnants: sand at the base, followed by gyttja and peat. At the base of the depression another extra component is present: calcium carbonate. This calcium carbonate could originate from the Cretaceous limestones under the Quaternary sediment, transported by groundwater seepage. This chalk is present throughout the entire gyttja layer.

7.3 LOI

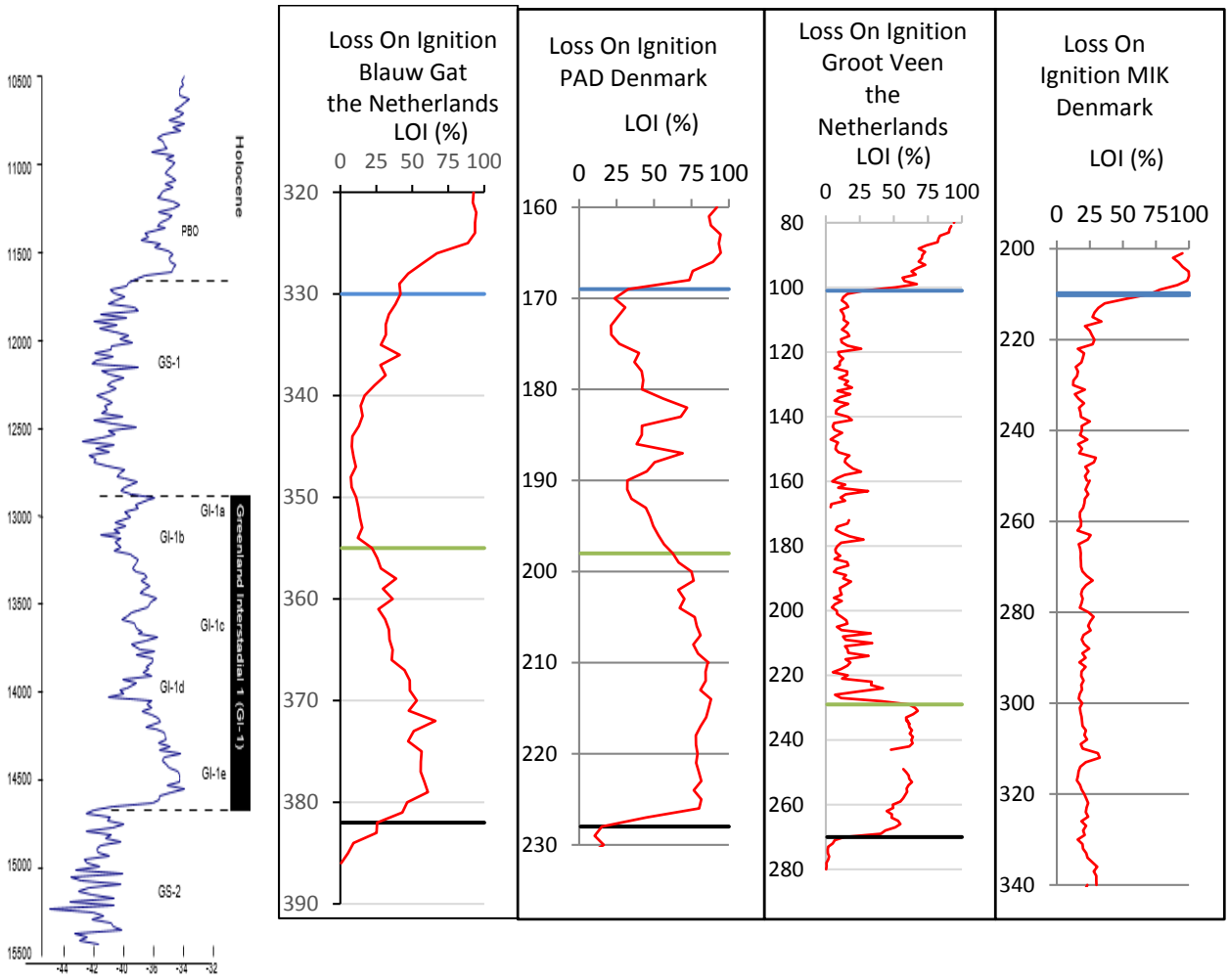

Figure 24: NGRIP oxygen-isotope curve (Hoek, 2009), compared with LOI circular depressions

Both the Dutch sites have very similar LOI characteristics, with increased LOI values during the Allerød and the Holocene, and lower LOI values during the Younger Dryas. The Blauw Gat LOI graph is more gradual and does not go from very high values to very low values, but gradually changes in between. The Groot Veen is very saw-tooth like and changes from one extreme to the other. The saw-tooth pattern could be due to aeolian influx, lowering the organic content.

The MIK LOI diagram does not look like the Dutch graphs. Only one climatic/chronological change could be identified; from colder times towards warmer times with very high organic matter content, which appears to be the Holocene. This confirms the lithology based genesis theory of a pitted sandar with kettle hole instead of pingo for the MIK depression. However, the PAD LOI diagram is similar to the Groot Veen diagram and very similar to the Blauw Gat diagram. The PAD diagram has all the same proportions as the Blauw Gat LOI diagram between the different zones and has the same smooth, gradual curve as the Blauw Gat. One of the smaller LOI peaks during the Allerød even seems to coincide in both graphs.

Comparing all these sites to the NGRIP oxygen isotope diagram shows many similarities (fig. 24). The LOI% of the Blauw Gat, Groot Veen and PAD diagrams follow the same pattern as the oxygen isotope curve, indicating the sensitivity of the LOI% to the climate as soon as vegetation developed. Moreover, this confirms the original age estimates of the zonation's.

7.4 Pollen diagrams

The pollen zones were mostly drawn based on the changes in Birch and Pine, changes in the ratio between the trees and upland herbs, and changes in occurrences of certain upland herb species.

The general trend of the infill of a pingo remnant follows the described pollen zones of Hoek (1997). The vegetation starts very barren, with many herbaceous plant communities and dwarf shrubs at the end of a cold, glacial period, after which birch and pine forest start to expand as the climate changes. As the temperature rises, vegetation starts to close up during the Allerød. The development is partly halted during the colder Younger Dryas, but birch forest expansion can continue again during the Holocene.

The Danish MIK pollen diagram does not evidently show the characteristics described by Hoek (1997) or Iversen (1973), indicating non deposition, disturbance of sediment or other deposits. This confirms the LOI and lithology inspired idea of different genesis, for example a kettle hole in a pitted sandar. The Danish PAD pollen diagram is slightly different compared to the Dutch pollen diagrams, but follows the description of Iversen (1973) of Late Quaternary pollen chronology.

7.5 Combining the results

Both the Dutch pingo remnant infillings are very similar in geomorphology, lithology, LOI and in pollen spectra. Although the pollen record and the LOI differ slightly, they indicate the same chronology. Since there was no thick continuous permafrost layer, no large areas underlain by coarse-grained sediment and no large number of thermokarst lakes that are easily drained nearby, these pingo remnants probably were open-system pingos.

The MIK depression is similar to the other depressions in morphology, but differs in lithology, LOI and in the pollen spectrum. Based on the coarse grained sand with limestone gravel, lack of gyttja, large amount of sand, lack of trends in the LOI and pollen diagram; the MIK depression is not a pingo remnant, but a dead ice hollow/kettle hole in a pitted sandar.

The PAD depression is similar to the Dutch pingo remnants in morphology, lithology, LOI and in pollen record. Therefore, the PAD depression is probably a pingo remnant. The specific type of pingo remnant is hard to determine, but is suspected to be a closed-system pingo; due to the Cretaceous limestone, thermokarst lakes could have developed. Moreover, large areas could have been underlain by coarse-grained sediment due to previous glacier advancement.

The LOI records and the pollen records do not show the exact same timing before transitioning from a warmer to a colder climate or vice versa. The timing is close and can be explained by Hoek (2000); when vegetation responds to climatic changes, the signal in biomass will generally follow afterwards, since the vegetation has to change first in order to get a biomass/organic fraction change. However, sometimes the organic fraction changes before the pollen signal. This can be due to slow migration of trees, lack of available nutrients or lack in the stability of the soil necessarily for forest establishment (Hoek, 2000).

8. Conclusions

This study aimed to make a comparison between some of the numerous pingo remnants in the Netherlands and circular depression in Denmark in order to discover if pingo remnants are present in Denmark. This was accomplished by analysing both the differences and similarities between the morphology and infill characteristics of circular depressions in Denmark and the pingo remnants in the Netherlands. The Danish circular depression were also compared with literature, in order to discover if the circular depressions had a different genesis than the pingo remnants. The hypothesis for this research was that some of the circular depressions in Denmark may be regarded as pingo remnants.

Is the timing of the decay of the pingos and the infill of the pingo remnants different on a local scale in the Netherlands in Drenthe?

Only two pingo remnants could be compared from Drenthe. The pollen signal, especially the tree signal of *Betula* and *Pinus*, was very similar throughout the entire infill. The upland herbs differ slightly; the upland herbs in the Blauw Gat appear to be more sensitive to climatic changes, making the pollen zones a bit more pronounced at this site. The LOI graphs have similar overall trends, through which climatic zones can be identified in both. However, the Groot Veen graph has more pronounced LOI minima and maxima than the Blauw Gat graph.

The moment of first infill appears to be the similar at both sites. The sites have sand deposits at the base of the infill, which are part of the original pingo structure before collapse, followed by gyttja deposits. Both have more artic/cold preferring pollen species at the sandy base, followed by warmer pollen associations. The LOI graphs confirm this trend.

Are the suspected pingo remnants in Denmark actual pingo remnants? If this is likely to be the case, how similar is the infill compared to the pingo remnants of the Netherlands? And if not, what are they?

The MIK site has the characteristic circular depression form of a pingo remnants, but that is where the similarities stop. Due to the infilling, both pollen, LOI and lithology (loam with small limestone gravel at the bottom), the circular depression does not to appear to have originated from the collapse of a pingo. Although not one of the alternative explanation is a perfect fit, the most likely alternative explanation is a pitted sandar with a crater kettle. This specific pitted sandar has thick diamiction layer in the pit, which would explain the infilling.

The PAD site has a similar morphology, similar lithological infill, similar pollen succession and a similar LOI curve as the Dutch sites. Moreover, calcium carbonate is also present in the lowest deposits. This supports the idea that the PAD depression might be a pingo remnant.

9. References

van Asch, N., Lutz, A. F., Duijkers, M. C., Heiri, O., Brooks, S. J., & Hoek, W. Z. (2012). Rapid climate change during the Weichselian Lateglacial in Ireland: Chironomid-inferred summer temperatures from Fiddaun, Co. Galway. *Palaeogeography, Palaeoclimatology, Palaeoecology*, 315, pp. 1-11.

Balyae, L. R. and Clymo, R. S. (2001). Feedback control on the rate of peat formation. *Proceedings of the Royal Society B: Biological Sciences,* 268, pp. 1315–1321.

Benn, D., & Evans, D. J. (2010). *Glaciers and Glaciations*. Hodder Arnold, pp. 531-534.

Berendsen, H. J. (2005). *Landschappelijk Nederland: de fysisch-geografische regio's.* Van Gorcum.

Björck, S. & Möller, P. (1987). Late Weichselian environmental history in southeastern Sweden during the deglaciation of the Scandinavian ice sheet. *Quaternary research*, 28 (1), pp. 1-37.

Björck, S. (1995). A review of the history of the Baltic Sea, 13.0-8.0 ka BP. *Quaternary International*, 27, pp. 19-40.

Bruijn, R. D. (2012). Pingo remnants in the northern Netherlands and north-western Germany.

Bryant, R. H., & Carpenter, C. P. (2011). Ramparted ground ice depressions in Britain and Ireland. *Periglacial Processes and Landforms in Britain and Ireland*, pp. 183.

Christiansen, H. H. (1995). Observations of open system pingos in a marsh environment, Mellemfjord, Disko, Central West Greenland. *Geografisk Tidsskrift-Danish Journal of Geography,* 95 (1), pp. 42-48.

Ehlers, J., & Gibbard, P. L. (2004). *Quaternary Glaciations-Extent and Chronology: Part I: Europe,* 2, Elsevier.

Faegri, K., & Iversen, J. (1964). Textbook of pollen analysis.

Flemal, R. C. (1976). Pingos and pingo scars: Their characteristics, distribution, and utility in reconstructing former permafrost environments. *Quaternary Research,* 6 (1), pp. 37-53.

French, H. M. (2007). *The periglacial environment*. John Wiley & Sons publication.

De Gans, W. (1988). Pingo scars and their identification. *Advances in Periglacial Geomorphology.* Wiley, New York, pp. 299-322.

Goudie, A. (2013). *Encyclopedia of geomorphology*, 1&2, Routledge's.

Grimm, E. C. (1992). TILIA and TILIA-graph: pollen spreadsheets and graphics programs. *Volume of abstract 8th International Palynological Congress, Aix-en-Provence*, pp. 56.

Gurney, S. D. (1998). Aspects of the genesis and geomorphology of pingos: perennial permafrost mounds. *Progress in Physical Geography,* 22(3), pp. 307-324.

Harris, S.A., French, H.M., Heginbottom, J.A., Johnston, G.H., Ladanyi, B., Sego, D.C. and van Everdingen, R.O. (1988). Glossary of permafrost and related ground-ice terms. *Permafrost Subcommittee, Associate Committee on Geotechnical Research, National Research Council of Canada, Ottawa, Technical Memorandum*, 142, pp. 156

Harris, C., & Ross, N. (2007). Pingos and pingo scars. *Encyclopedia of Quaternary Science,* 2, pp. 2200-2207.

Heiri, O., Lotter, A. F., & Lemcke, G. (2001). Loss on ignition as a method for estimating organic and carbonate content in sediments: reproducibility and comparability of results. *Journal of paleolimnology,* 25 (1), pp. 101-110.

Hoek, W. Z. (1997). *Atlas to Palaeogeography of Lateglacial vegetations: maps of Lateglacial and Early Holocene landscape and vegetation in The Netherlands, with an extensive review of available palynological data.* Koninklijk Nederlands Aardrijkskundig Genootschap.

Hoek, W.Z., Bohncke, S.J.P., 2001. Oxygen-isotope wiggle matching as a tool for synchronising ice-core and terrestrial records over Termination 1. *Quaternary Science Reviews,* 20, pp. 1251–1264

Hoek, W. Z. (2009) Bølling-Allerød Interstadial. *Encyclopedia of paleoclimatology and ancient environments.* Springer Netherlands, pp. 100-103.

Houmark-Nielsen, M. (1987). Pleistocene stratigraphy and glacial history of the central parts of Denmark. *Bulletin of the Geological Society of Denmark*.

Houmark-Nielsen, M. (1999). A lithostratigraphy of Weichselian glacial and interstadial deposits in Denmark. *Bulletin of the Geological Society of Denmark*, 46 (1), pp. 101-114.

Houmark-Nielsen, M., & Henrik Kjær, K. (2003). Southwest Scandinavia, 40–15 kyr BP: palaeogeography and environmental change. *Journal of Quaternary Science*, *18* (8), pp. 769-786.

Houmark-Nielsen, M. (2004). The Pleistocene of Denmark: a review of stratigraphy and glaciation history. *Developments in Quaternary Sciences*, 2, pp. 35-46.

Houmark-Nielsen, M. (2007). Extent and age of Middle and Late Pleistocene glaciations and periglacial episodes in southern Jylland, Denmark. *Bulletin of the Geological Society of Denmark*, 55 (1), pp. 9-35.

Iversen, J. (1973). The development of Denmark's nature since the last glacial. *Geological Survey of Denmark. V. Series*, 7C.

Kuhry, P., Dorrepaal, E., Hugelius, G., Schuur, E. A. G., & Tarnocai, C. (2010). Potential remobilization of belowground permafrost carbon under future global warming. *Permafrost and Periglacial Processes,* 21 (2), pp. 208-214.

Landvik, J.Y., Bondevik, S., Elverhøi, A., Fjeldskaar, W., Mangerud, J.A.N., Salvigsen, O., Siegert, M.J., Svendsen, J.I. and Vorren, T.O. (1998). The last glacial maximum of Svalbard and the Barents Sea area: ice sheet extent and configuration. *Quaternary Science Reviews*, 17 (1), pp. 43-75.

Mackay, J. R. (1962). Pingos of the Pleistocene Mackenzie delta area*. Geographical Bulletin,* 18 (2), pp. 1-63.

Mackay, J. R. (1972). The world of underground ice. *Annals of the Association of American Geographers,* 62 (1), pp. 1-22.

Mackay, J. R. (1973). The growth of pingos, western Arctic coast, Canada. *Canadian Journal of Earth Sciences,* 10(6), pp. 979-1004.

Mackay, J. R. (1979). Pingos of the Tuktoyaktuk Peninsula area, Northwest territories*. Géographie physique et Quaternaire,* 33 (1), pp. 3-61.

Mackay, J.R. (1987). Some mechanical aspects of pingo growth and failure, western Arctic coast, Canada. *Canadian Journal of Earth Sciences*, 24, pp. 1108-1119.

Mackay, J. R. (1998). Pingo growth and collapse, Tuktoyaktuk Peninsula area, western Arctic coast, Canada: A long-term field study. *Géographie physique et Quaternaire,* 52(3), pp. 271-323.

Mollard, J. D. (2000). Ice-shaped ring-forms in Western Canada: their airphoto expressions and manifold polygenetic origins. *Quaternary International,* 68, pp. 187-198.

Mortensen, M. F., Birks, H. H., Christensen, C., Holm, J., Noe-Nygaard, N., Odgaard, B. V., Olsen, J., Rasmussen, K. L. (2011). Lateglacial vegetation development in Denmark–new evidence based on macrofossils and pollen from Slotseng, a small-scale site in southern Jutland. *Quaternary Science Reviews*, 30 (19), pp. 2534-2550.

De Mulder, E. F., Geluk, M. C., Ritsema, I., Westerhoff, W. E., & Wong, T. E. (2003). De ondergrond van Nederland. *Geologie van Nederland*, 7.

Muller, S.W. (1945). Permafrost or permanently frozen ground and related engineering problems. *Military Intelligence Division, Office, Chief of Engineers, U.S. Army, Washington, D.C*, pp. 231.

Müller, F. (1959). Beobachtungen Uber Pingos. Detailuntersuchungen in Ostgronland und in der kanadischen Arktis. *Aeddelelser om Gronlalld.*

Müller, F. (1963). Observations on pingos (Beobachtungen iiber Pingos). *Canada National Research Council Technical Translation*, 1073, pp. 117.

Ozawa, H. (1997). Thermodynamics of frost heaving: A thermodynamic proposition for dynamic phenomena. *Physical Review E,* 56 (3), pp. 2811.

Pedersen, S. A. S. (1989). Jordagskort over Danmark 1:200000, Nordjylland. *Danmarks Geologiske Undersogelse.*

Pissart, A., & French, H. M. (1976). Pingo investigations, north-central Banks Island, Canadian Arctic. *Canadian Journal of Earth Sciences,* 13 (7), pp. 937-946.

Porsild, A. E. (1938). Earth mounds in unglaciated arctic northwestern America. *Geographical Review*, pp. 46-58.

Ruiter, A. S. (2012). Relict pingos and permafrost.

Seppälä, M. (1972). The term "palsa". *Zeitschrift für Geomorphologie NF*, 16, pp. 463.

Seppälä, M. (1988). Palsas and related forms. *Advances in periglacial geomorphology*, pp. 247-278.

Svendsen, J.I., Alexanderson, H., Astakhov, V.I., Demidov, I., Dowdeswell, J.A., Funder, S., Gataullin, V., Henriksen, M., Hjort, C., Houmark-Nielsen, M. and Hubberten, H.W. (2004). Late Quaternary ice sheet history of northern Eurasia. *Quaternary Science Reviews*, 23 (11), pp. 1229-1271.

Svensson, H. (1969). A type of circular lake in northernmost Norway. *Geografiska Annaler*, 51A, pp. 112.

Ter Wee, M. W. (1966). *Toelichtingen bij de Geologische kaart van Nederland1:50000, Steenwijk Oost (16 O).* Geologische Stichting, Afdeling Geologische Dienst, Haarlem.

Yoshikawa, K (2013). Pingos 8.18. *Reference Module in Earth Systems and Environmental Sciences, from Treatise on Geomorphology,* 8, pp. 274-297.

10. Appendices

10.1 Pollen preparation guidelines (Dutch)

Werkvoorschrift Pollenpreparatie UU-FG

In met name stap 2 worden sterke zuren gebruikt, raadpleeg vooraf de fact-sheets over de te gebruiken chemicaliën. Raadpleeg bij onzekerheid altijd Wim Hoek

1 Ontkalken en uitlogen

- Ca. 0.3 cm^3 materiaal in 15 ml centrifugebuis, aanvullen met aqua dest. tegen oxidatie.
- Bij kalkhoudend materiaal: uitzuren met 5% azijnzuur, daarna 2 maal uitwassen met aqua dest. om zuur te verwijderen (= 2x: aanvullen aq. dest, vortexen, centrifugeren 1 min bij 1700 r.p.m. en decanteren).
- (Eventueel Lycopodium toevoegen, tbv absolute pollendiagrammen). 5 ml KOH 5% toevoegen om humusverbindingen te verwijderen. Dop reageerbuis niet helemaal dicht draaien voor ontsnapping gassen in stoof.
- 60 minuten verwarmen in stoof bij 70 °C.
- Vortexen totdat goed gemixt, dan zeven over 200 mu, direct in 15 ml centrifugebuis.
- 2 maal uitwassen met aqua dest. om KOH te verwijderen (= 2x: aanvullen met aq. dest, vortexen, centrifugeren 1 min bij 1700 r.p.m. en decanteren).

2 Acetolyse (uit te voeren door gekwalificeerd medewerker)

NB zuren altijd afgieten in speciaal zuurvat

- 2 maal uitwassen met ijsazijn om water te verwijderen (aanvullen tot 5 ml).
- Acetolyse mengsel: 9 delen Azijnzuuranhydride + 1 deel H_2SO_4. (bij 48 samples is dit 180 ml + 20 ml)
- Ca 4 ml acetolyse mengsel toevoegen en mengen. 5-10 min verwarmen bij 100° C. in warmtebad. Tussendoor (na het bereiken van 100°) éénmaal vortexen.
- Centrifugeren, acetolyse mengsel afgieten in speciaal zuurvat.
- Tweemaal uitwassen met aqua dest. om zuur te verwijderen in andere afvalbeker dan acetolyse (= 2x: aanvullen met aq. dest, vortexen, centrifugeren 1 min bij 1700 r.p.m. en decanteren).

3 Zware vloeistof scheiding

NB Resten zware vloeistof altijd afgieten in plastic wasfles voor zware vloeistof.

- Vortexen of schudden mengsel, centrifugeren, afgieten.
- 4 ml zware vloeistof (Natrium-polywolframaat met d=2.0) toevoegen. Vortexen om goed te mengen.
- 15 minuten bij 1700 r.p.m. centrifugeren om te scheiding op soortelijk gewicht.
- Kraag decanteren in conische centrifugebuis, deze aanvullen met aqua dest tot 10 ml, schudden en 5 minuten uitcentrifugeren bij 1700 r.p.m. De gedecanteerde reageerbuis aanvullen met 4 ml zware vloeistof, vortexen en 15 min uitcentrifugeren bij 1700 r.p.m. (buizen kunnen ook bij elkaar in de centrifuge, langer centrifugeren niet erg voor conische reageerbuizen in dit geval).
- Eerst conische reageerbuis decanteren in plastic wasfles voor zware vloeistof, dan herhalen: weer rest van kraag afgieten normale reageerbuis in de conische buis, deze aanvullen met aqua dest tot 10 ml, deze schudden en 5 minuten uitcentrifugeren bij 1700 r.p.m. Restant normale reageerbuis aanvullen met aq. Dest, vervolgens afgieten in andere plastic fles voor zware vloeistof. En reageerbuis bij de vieze was leggen.
- Conische reageerbuis decanteren en aq. dest toevoegen, schudden, en 5 minuten uitcentrifugeren bij 1700 r.p.m

4 Afwerken

- Als stap 3 even geleden: Hierna ca. 2 à 3 maal uitwassen met water na 1 min. bij 1700 r.p.m.
- Na decanteren1.5 ml Alcohol toevoegen.
- Klein beetje vortexen en overbrengen in Eppendorf cup.
- Eppendorf cup vortexen, cup openen en in special centrifuge bakken doen, uitcentrifugeren voor 2 min by 1700 r.p.m.
- Decanteren en glycerine toevoegen (evenveel glycerine als monster).
- Eppendorf cups open laten en residu een nacht in stoof bij max.70 °C.

5 Preparaat maken

NB: Pollenslide doos altijd rechtop houden

- Met botte houte tandenstoker glycerine en pollen mixen
- Op objectglaasje details monster schrijven
- Druppel van ong 1x2 mm op objectglaasje aanbrengen met tandenstoker
- Objectglaasje op wartmeplaat leggen en voorzichtig dekglaasje er op leggen (terwijl 1 kant wordt neergezet op objectglas, andere kant rustig laten vallen over pollen).
- Snel kaarswax staaf pakken en aan 1 kant dekglaasje deze heen en weer bewegen.
- Wax hoort om pollenmonster heen te trekken en lucht weg te duwen, mag geholpen worden door aanduwen dekglaasje met tandenstoker.
- Objectglas verwijderen van warmteplaat en laten drogen tot wax wittige gloed krijgt. Deze pollen slide vervolgens in pollen slide doosje overbrengen, die altijd rechtop moet staan om verplaatsen van pollen tegen te gaan.

10.2 Coring descriptions

Blauw gat			
name	x coordinate	y coordinate	
A-I2	209134	542947	
depth in cm	**description**		
306-316	young moss peat, brown		
316-349	very compacted sandy sedge&moss peat, brc		
349-359	sandy gyttja, brown		
359-370	organic gyttja, black/dark brown		
370-380	organic gyttja, dark brown		
380-387	gyttja, brown		
387-395	sandy gyttja, grey-brown		
395-405	fine sand with a lot of organic material, brow		
405-406	fine sand, grey		
name	x coordinate	y coordinate	
B-I2	209134	542947	
depth in cm	**description**		
351-382	sandy moss and sedge peat, brown		
382-396	very organic gyttja, black-dark brown		
396-404	organic gyttja with moss, orange-brown		
404-413	organic gyttja, brown		
413-419	sandy gyttja, brown		
419-426	fine sand, yellow-grey, with organic remains		
426-448	fine sand, yellow-grey, with gravel		
* drilling hiatus, coring goes to 450			
name	x coordinate	y coordinate	
C-IA	209143	542922	
depth in cm	**description**		
160-190	amorphous peat, brown		

name	x coordinate	y coordinate	
C-IB	209143	542922	
depth in cm	**description**		
190-224	sedge peat, black-brown		
224-290	sedge peat, orange-brown		
name	x coordinate	y coordinate	
C-IIA	209143	542922	
depth in cm	**description**		
221-224	amorphous peat, black		
224-259	sedge peat, brown		
259-278	sedge peat, dark brown		
278-286	sedge&moss peat, brown		
name	x coordinate	y coordinate	
C-IIB	209143	542922	
depth in cm	**description**		
286,5-322,5	sedge peat, brown		
322,5-324,5	sandy peat, black		
324,5-362	sandy peat, grey-brown		
362-379	sandy gyttja, dark brown		
379-385	sandy gyttja, light brown		
385-386,5	fine sand, yellow and organic matter		

Groote veen

x coordinate	y coordinate
216275	547451

depth in cm	description
0-20	peaty fine sand, brown
20-30	clean, yellow-brown fine sand with organic black spots
30-40	humic fine sand, light brown
40-100	humic fine sand, brown
100-140	fine sand, brown

x coordinate	y coordinate
216269	547465

depth in cm	description
0-30	loose, young moss peat with water, orange-brown
30-70	sandy peat, dark brown, almost black (almost completly oxidized)
70-100	humic sand, brown
100-155	sandy peat, brown, with decreasing sand concentration towards 155 and increasing moss concentration
155-170	plant remains, moss and towards 170 gravel pieces, brown
170-	fine sand yellow-brown

x coordinate	y coordinate
216266	547477

depth in cm	description
0-40	sandy peat, brown
40-110	amorphous peat, dark brown, with some sedge and moss at 100 cm
110-150	peaty sand with sand lenses, brown
150-180	strong sandy mosspeat with sand lenses, orange-brown
180-200	sandy moss peat, orange-brown
200-250	yellow-grey fine sand with plant remains

x coordinate	y coordinate
216258	547481

depth in cm	description
0-60	sandy peat, amorphous, dark brown to black
60-100	amorphous peat, brown-black
100-110	amorphous peat, brown
110-120	sandy peat, brown
120-150	sandy moss peat, light brown
150-175	sandy moss peat with sand lenses, light brown
175-200	sandy moss peat with salix leaf, gyttja achtig
200-215	gyttja, fine detritus, brown-grey, potamogeton seed
215-220	coarse detritus gyytja, brown-grey, menyantes seed
220-230	fine sand, yellow-brown, with moss layer at 225

x coordinate	y coordinate							
216238	547522							
depth in cm	**description**							
0-90	sandy peat, amorphous, dark brown							
90-120	peaty sand, brown							
120-230	peaty sand, brown, with sand lenses, moss							
230-240	sandy peat, with a sand layer and a moss layer							
240-267	gyttja, brown-grey							
267-270	mix of moss peat, sand and carex seeds.							
270-273	leaves and organic material, dark-brown/black							
273-300	fine sand, grey							
x coordinate	y coordinate							name
216243	547522							
depth in cm	**description**	*** depth taken from water surface**						
0-20	water							GV15-I
20-31	recent amorphous peat, brown							GV15-I
31-49	sandy, amorphous peat, rooted, black/dark brown							GV15-I
49-80	amorphous peat, rooted, recognizable organic matter, dark brown							GV15-I
80-100	sandy, amorphous peat, black							GV15-II
100-108	peaty sand, black							GV15-II
108-131	humic sand, brown							GV15-II
131-168	humic sand, brown, with sand lenses							GV15-II
170-200	humic sand, light brown, organic material, moss lens at 183.5, sand lens 176							GV15-III
200-205	peaty sand, brown, with sand lenses							GV15-III
205-206	moss lens orange-brown							GV15-III
206-228	peaty sand, brown, with 'pure' sand lenses at 225-226, 217-219							GV15-III
228-235	sandy gyttja, brown							GV15-III
200-204	peaty sand, brown							GV15-IV
204-206	moss, orange-brown							GV15-IV
206-228	peaty sand, brown, sand lenses at 225-226, 217-219							GV15-IV
228-243	sandy gyttja, brown							GV15-IV
239-256	a bit sandy gyttja, brown							GV15-V
256-262,5	sandy gyttja, brown							GV15-V
262,5-263,5	organic belt, black							GV15-V
263,5-264,5	sandy gyttja, brown							GV15-V
264,5-265	humic sand, light brown							GV15-V
248-259	a bit sandy gyytja, brown							GV15-VI
259-266	organic belt, black							GV15-VI
266-269	a bit sandy gyytja, brown							GV15-VI
269-277	humic fine sand, light brown, with organic matter (black)							GV15-VI
277-280	fine sand, grey with organic material							GV15-VI

x coordinate	y coordinate				
216230	547534				
depth in cm	**description**				
0-110	sandy peat, dark brown				
110-190	peaty sand, brown, with fine sand lenses				
190-210	sandy moss peat, brown				
210-250	gyttja, brown-grey				
250-255	sandy moss peat, orange-brown				
255-280	fine sand, grey				
x coordinate	y coordinate				
216214	547572				
depth in cm	**description**				
0-130	peaty sand, brown				
130-140	gyttja, grey-brown				
140-141	moss layer, brown-orange				
141-150	organic material with some fine sand,moss and peat				
150-160	fine sand				

MIK15-					
name	x coordinate	y coordinate			
MIK15-1	509482	6136445			
depth in cm	**description**				
0-60	young peat, black				
60-80	moss peat, orange-brown				
80-90	sedge peat, black, lot of organics, very intact				
90-120	humic sand, brown-grey				
120-125	humic sand, orange-brown, more organics, almost gyttja				
125-140	humic sand, brown-grey, sand lens 132				
140-170	fine sand, green-grey				
170-230	sandy loam, limestone pieces, gravel				
name	x coordinate	y coordinate			
MIK15-2	509482	6136445			
depth in cm	**description**				
0-50	young peat, black				
50-65	moss peat, roots all through, brown-orange				
65-75	sedge peat, black-brown				
75-200	moss peat, brown-orange, charcoal layer 130				
200-210	leaf remains				
210-224	humic sand, light brown				
224-238	little bit humic sand, grey-brown				
238-310	humic sand, light brown, 307 sand lens				
310-345	humic sand, grey-brown				
345-360	abrupt change to blue-grey sand				
name	x coordinate	y coordinate			
MIK15-3	509482	6136445			
depth in cm	**description**				
0-50	peat, brown				
50-85	peat, brown-black				
85-180	peat, brown				
180-260	moss peat, orange-brown				
260-390	humic sand				

PAD15-				
name	x coordinate	y coordinate		
PAD15-1	519884	6082380		
depth in cm	**description**			
0-120	amorpuous peat, dark brown			
120-210	peat, brown and pieces of wood			
210-235	sedge peat, brown			
235-330	humic sand and gravel			
330-360	very humic sand			
name	x coordinate	y coordinate		
PAD15-2	519875	6082384		
depth in cm	**description**			
0-120	amorphous peat, brown			
120-150	wood peat, brown			
150-175	sandy peat with gravel			
175-280	sedge peat, brown, moss			
280-300	gyttja, grey-brown			
300-310	a bit humic sand, chalk, licht brown-grey			
310-320	sandy gyttja, chalk, brown-grey			
320-	coarse sand, grey			
name	x coordinate	y coordinate		
PAD15-3				
depth in cm	**description**			
170-180	disturbed peat			
180-213	orange/brown moss, with pieces of sedge			
213-227	dark brown amorphous peat			
227-230	dark brown/grey, peaty gyttja			
230-236	light brown chalcky gyttja			
236-242	grey, chalck gyttja			
242-250	dark grey chalck gyttja			

10.3 Complete LOI graphs

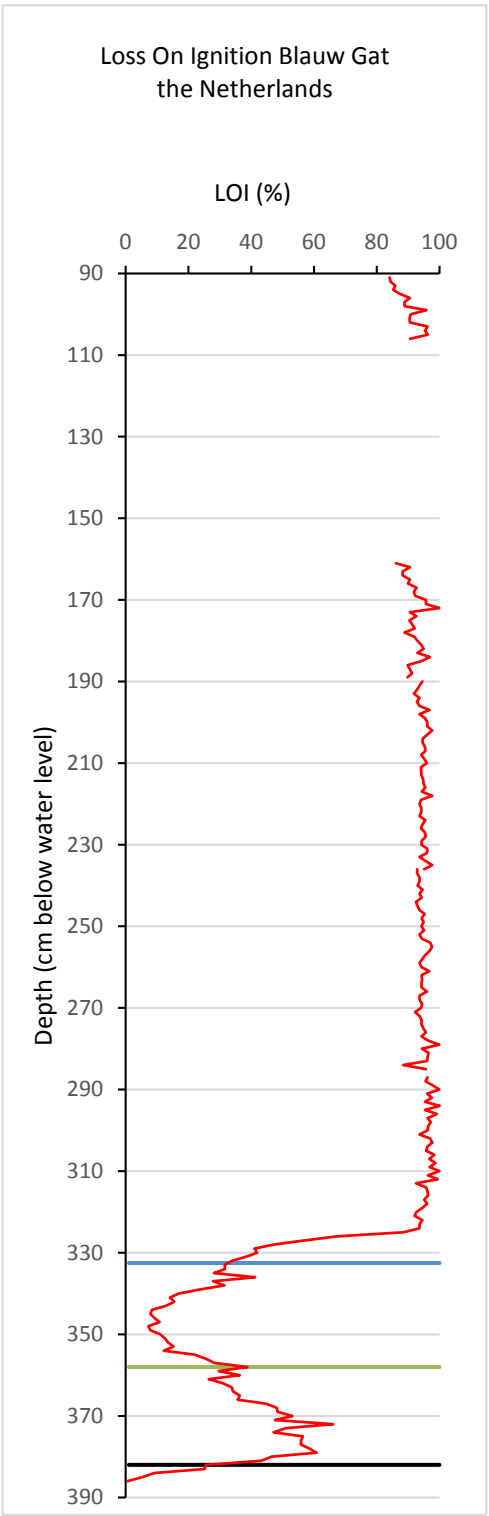

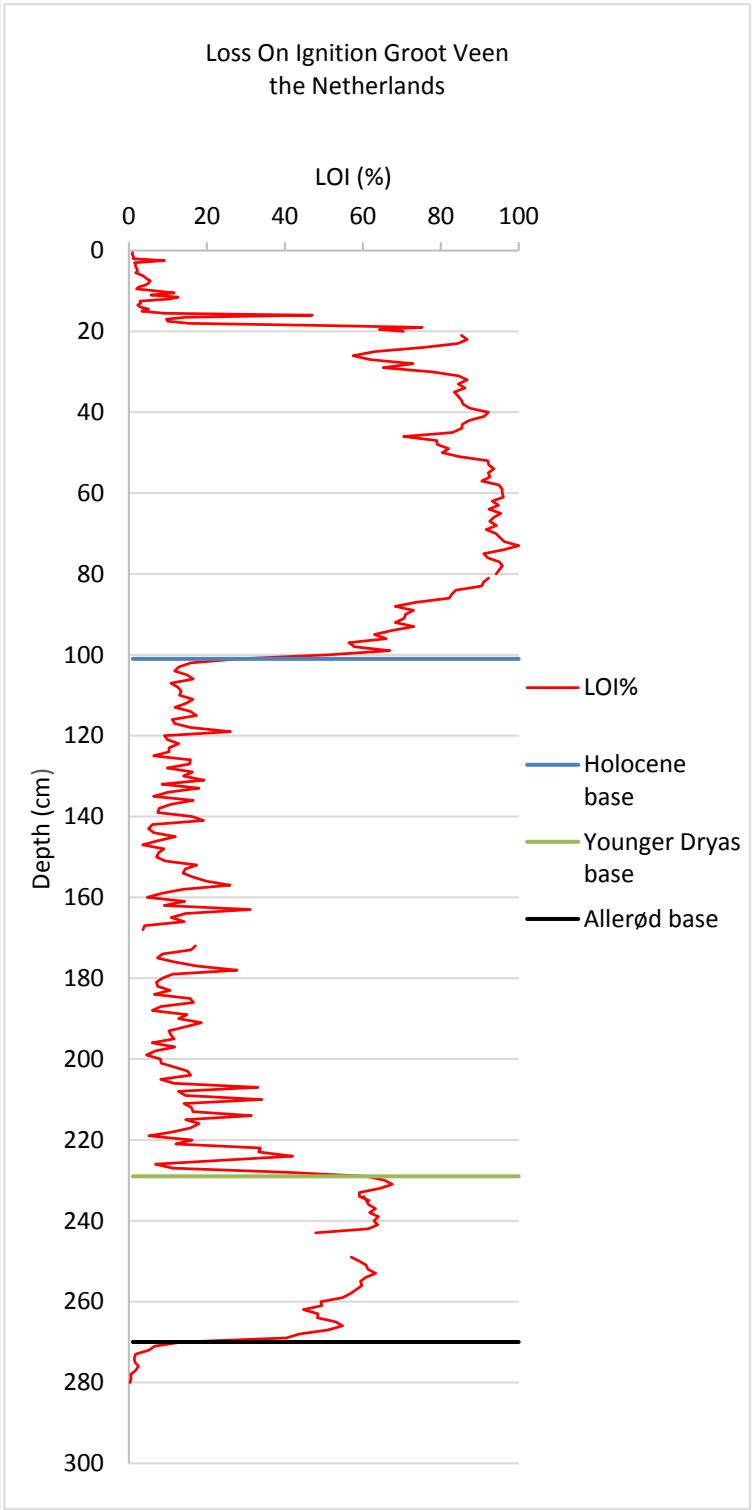

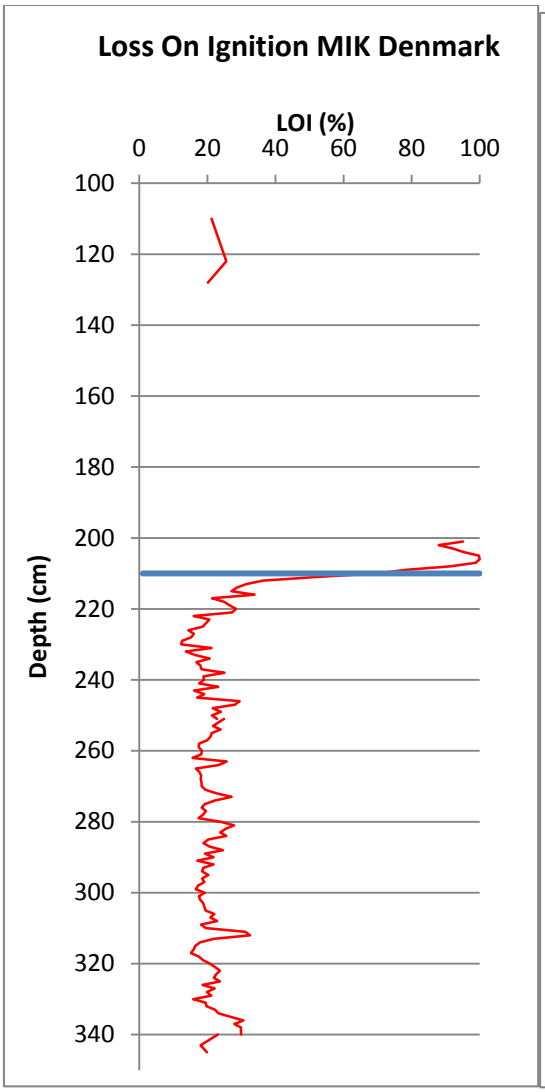
Loss On Ignition MIK Denmark
LOI (%)
0
20
40
60
80
100
Depth (cm)
100
120
140
160
180
200
220
240
260
280
300
320
340

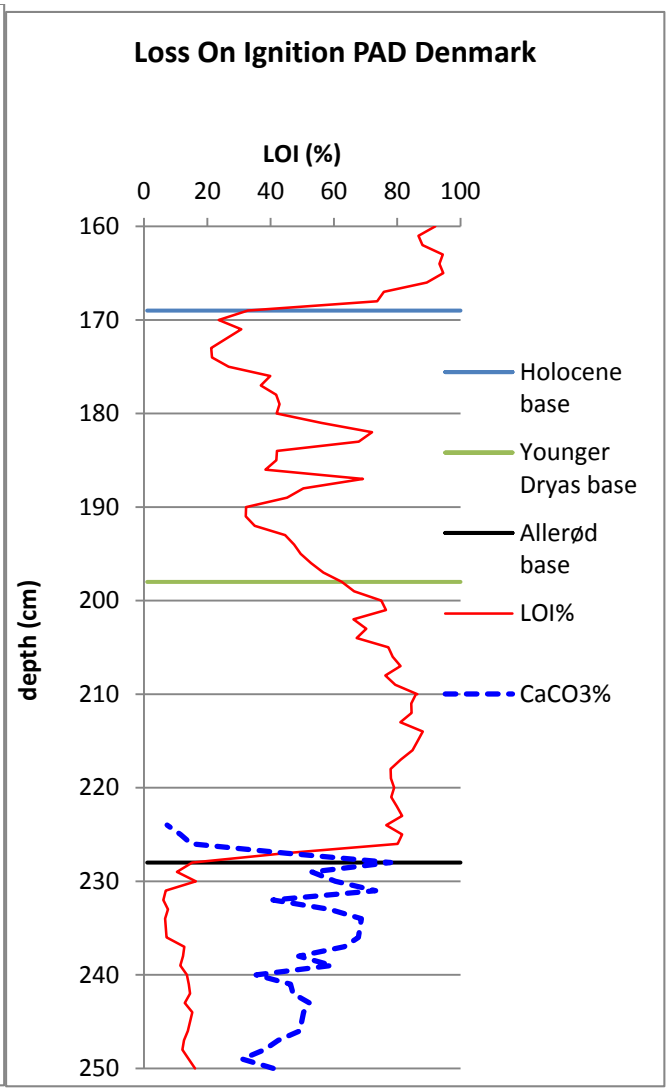
Loss On Ignition PAD Denmark
LOI (%)
0
20
40
60
80
100
depth (cm)
160
170
180
190
200
210
220
230
240
250
Holocene base
Younger Dryas base
Allerød base
LOI%
CaCO3%

10.4 Complete pollen diagrams

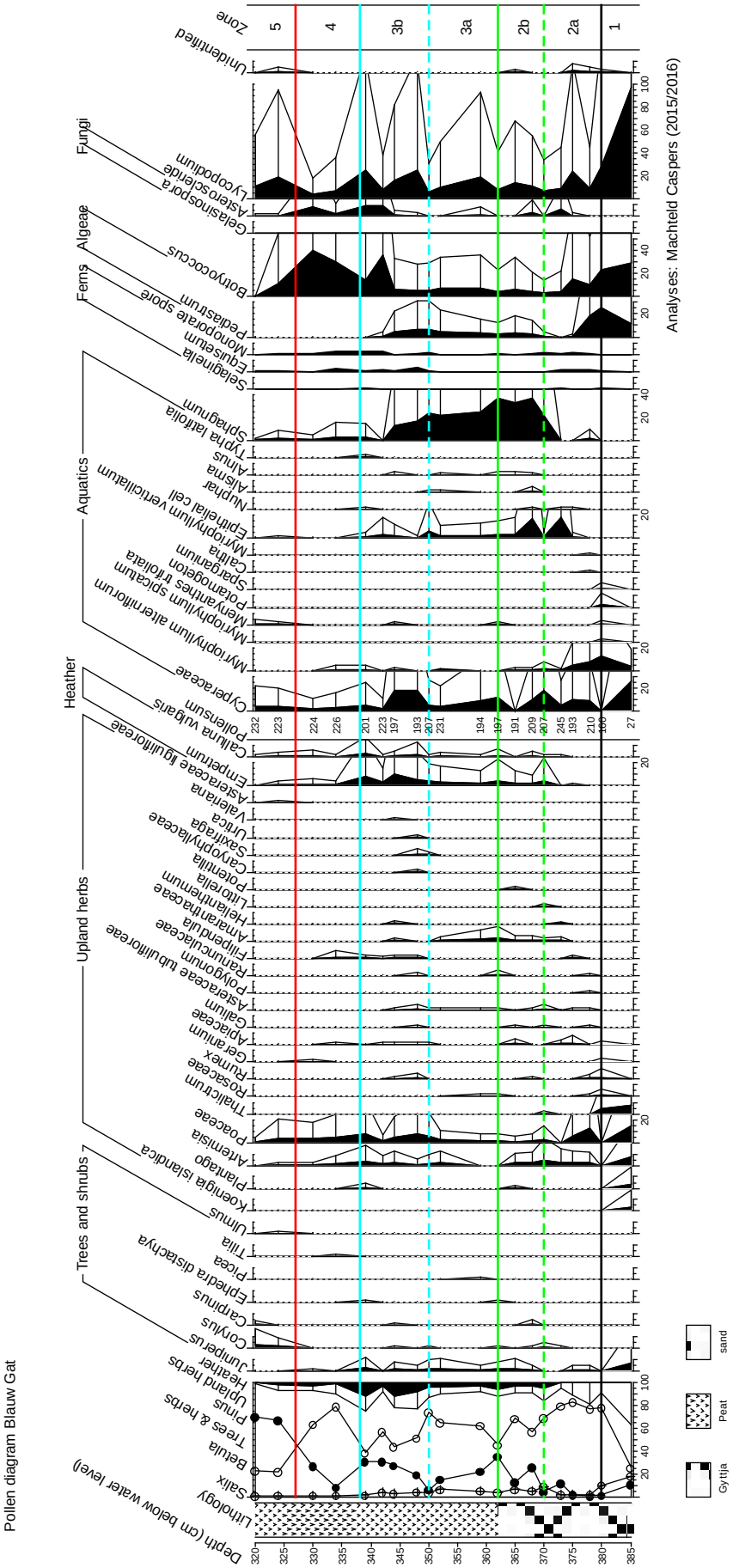

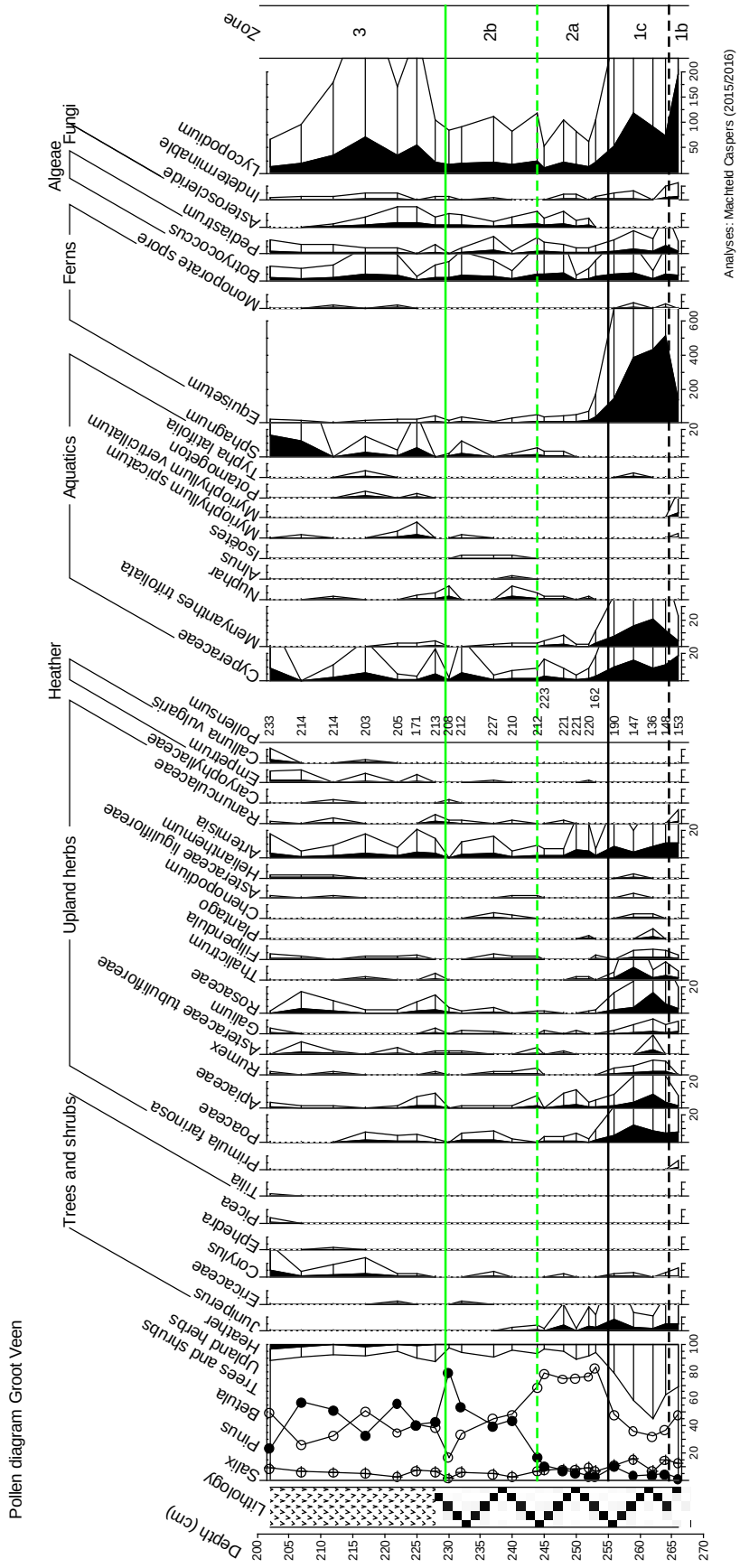
Pollen diagram Groot Veen
Depth (cm)
Lithology
Salix
Pinus
Betula
Trees and shrubs
Upland herbs
Heather
Juniperus
Ericaceae
Corylus
Ephedra
Picea
Tilia
Primula farinosa
Poaceae
Apiaceae
Rumex
Asteraceae tubuliflorae
Galium
Rosaceae
Thalictrum
Filipendula
Plantago
Chenopodium
Asteraceae liguliflorae
Helianthemum
Artemisia
Ranunculaceae
Caryophyllaceae
Empetrum
Calluna vulgaris
Pollensum
Cyperaceae
Menyanthes trifoliata
Nuphar
Alnus
Isoetes
Myriophyllum spicatum
Myriophyllum verticillatum
Potamogeton
Typha latifolia
Sphagnum
Equisetum
Monoporate spore
Botryococcus
Pediastrum
Asteroscleriid
Indeterminable
Lycopodium
Aquatics
Ferns
Algeae
Fungi
Zone
3
2b
2a
1c
1b
Analyses: Machteld Caspers (2015/2016)
Sand
Gyttja
Peat

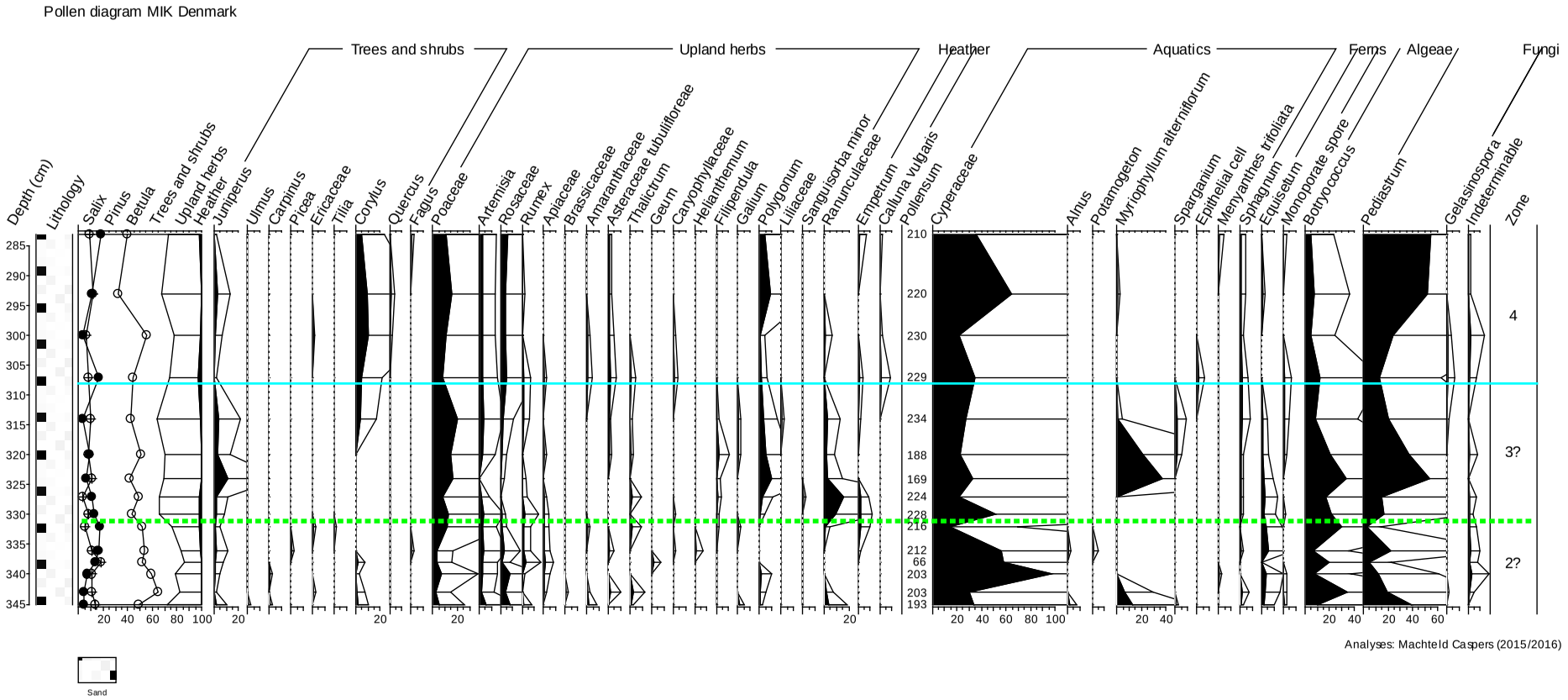
Pollen diagram MIK Denmark
Trees and shrubs
Upland herbs
Heather
Aquatics
Ferns
Algeae
Fungi
Depth (cm)
Lithology
Salix
Pinus
Betula
Trees and shrubs
Upland herbs
Heather
Juniperus
Ulmus
Carpinus
Picea
Ericaceae
Tilia
Corylus
Quercus
Fagus
Poaceae
Artemisia
Rosaceae
Rumex
Apiaceae
Brassicaceae
Amaranthaceae
Asteraceae tubuliflroeae
Thalictrum
Geum
Caryophyllaceae
Hellanthemum
Filipendula
Galium
Polygonum
Liliaceae
Sanguisorba minor
Ranunculaceae
Empetrum
Calluna vulgaris
Pollensum
Cyperaceae
Alnus
Potamogeton
Myriophyllum alterniflorum
Sparganium
Epithelial cell
Menyanthes trifoliata
Sphagnum
Equisetum
Monoporate spore
Botryococcus
Pediastrum
Gelasinospora
Indeterminable
Zone
285
290
295
300
305
310
315
320
325
330
335
340
345
210
220
230
229
234
188
169
224
228
216
212
66
203
203
193
4
3?
2?
20 40 60 80 100
20
20
20
20 40 60 80 100
20 40
20 40
20 40 60
Sand
Analyses: Machteld Caspers (2015/2016)

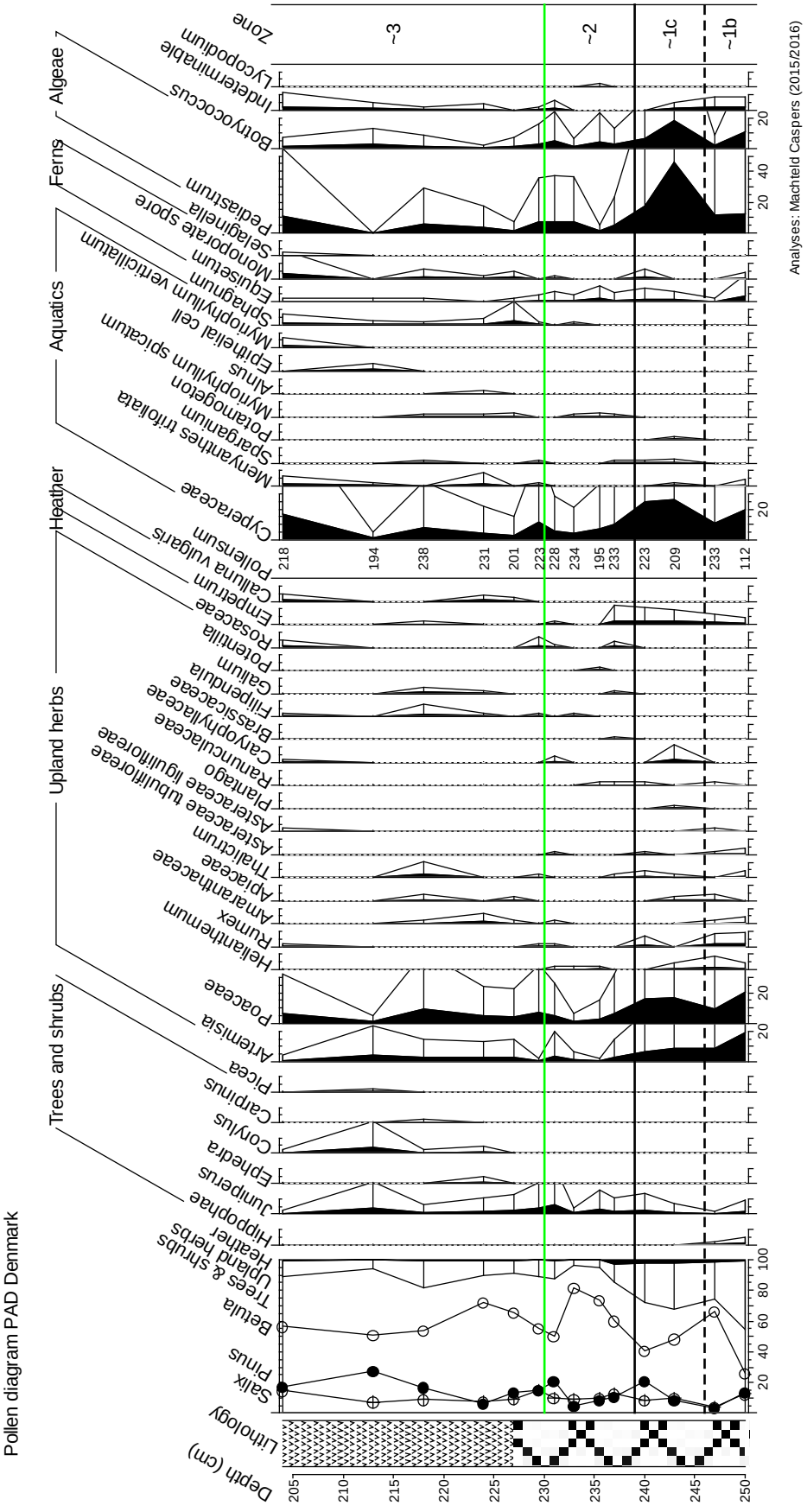
Pollen diagram PAD Denmark
Depth (cm)
Lithology
Sand
Gyttja
Peat
Zone
~3
~2
~1c
~1b
Trees and shrubs
Upland herbs
Heather
Aquatics
Ferns
Algeae
Salix
Pinus
Betula
Trees & shrubs
Upland herbs
Heather
Hippophae
Juniperus
Ephedra
Corylus
Carpinus
Picea
Artemisia
Poaceae
Helianthemum
Rumex
Armeranthaceae
Apiaceae
Thalictrum
Asteraceae tubuliflorae
Asteraceae liguliflorae
Plantago
Ranunculaceae
Caryophyllaceae
Brassicaceae
Filipendula
Galium
Potentilla
Rosaceae
Empetrum
Calluna vulgaris
Pollensum
Cyperaceae
Menyanthes trifoliata
Sparganium
Potamogeton
Myriophyllum spicatum
Alnus
Epithelial cell
Myriophyllum verticillatum
Sphagnum
Equisetum
Monoporate spore
Selaginella
Pediastrum
Botryococcus
Indeterminable
Lycopodium
Analyses: Machteld Caspers (2015/2016)

10.5 Pollen diagram Rijks Geologische Dienst